Personal Account

THE CHEMICAL RECORD

DOI: 10.1002/tcr.202100012

# Heteroditopic Calix[6]arene Based Intervowen and Interlocked Molecular Devices

Gianpiero Cera,[a] Arturo Arduini,*[a] Andrea Secchi,[a] Alberto Credi,*[b, c] and Serena Silvi[d]

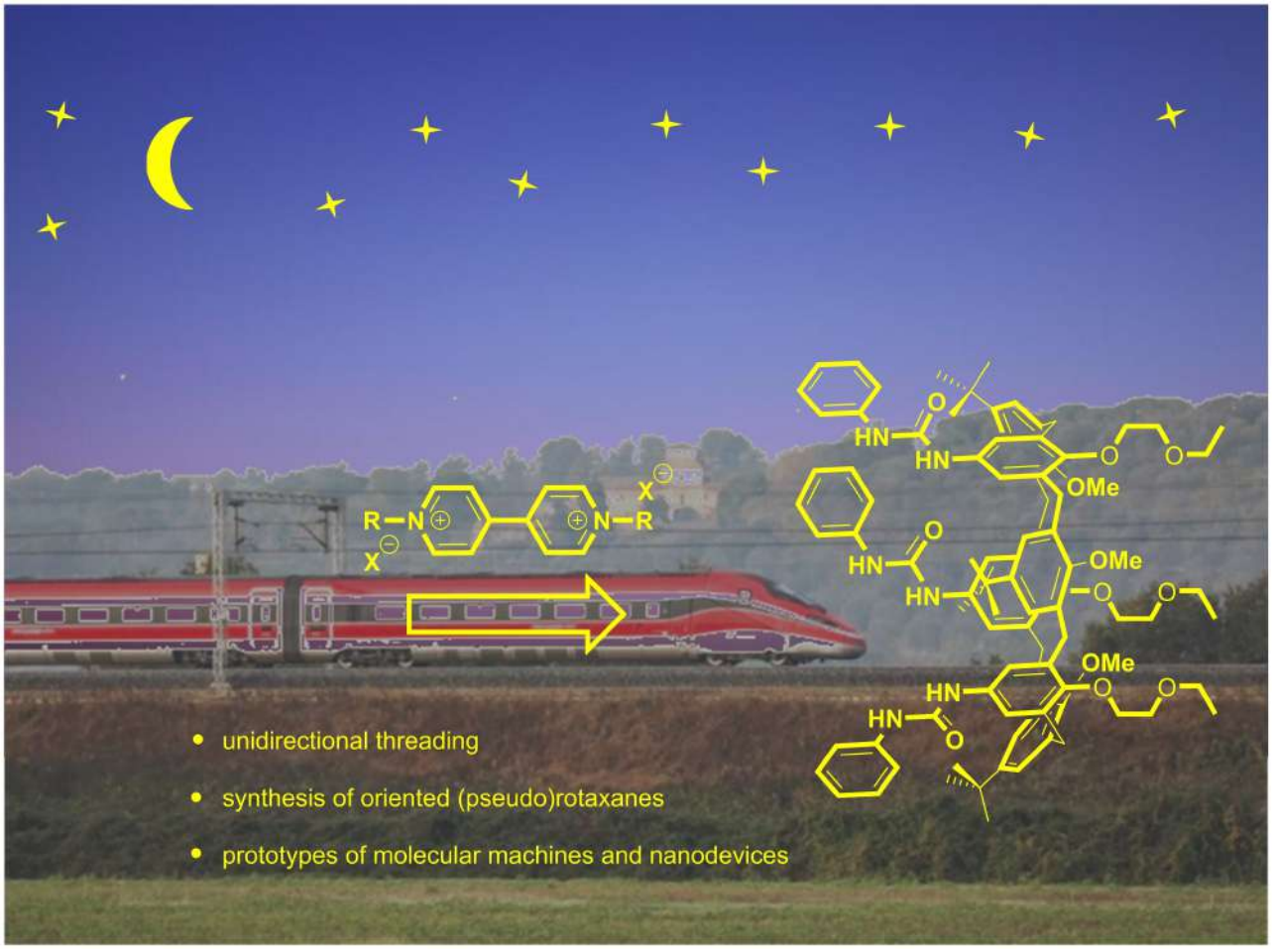


  

**Abstract:** Since the dawn of supramolecular chemistry, calixarenes have been employed as platforms onto which functional groups and binding sites can be loaded in a regio- and stereocontrolled manner for the recognition of charged and neutral species. Despite their wider annulus, potentially suitable to bind larger guests, the larger members of the calixarene series have been relatively less employed, mainly because of the synthetic difficulties to control their conformational flexibility and their regioselective functionalization. In this account, we will present the achievements gained during the last two decades on the use of the calix[6]arene as a platform to build-up structures in which the macrocycle acts as a wheel for the synthesis of oriented (pseudo)rotaxanes. We also account on how these calix[6]arene hosts affect the reactivity or spectroscopic properties of their bound guests.

**Keywords:** Calix[6]arenes, Mechanical Interlocked Molecules, (Pseudo)rotaxanes, Catenanes, Molecular Machines

## 1. Introduction

Every chemical species is endowed with a heritage of structural and chemical information responsible for its physical and chemical properties. The reading of this information offers powerful guidelines to govern chemical processes and design and synthesize molecular receptors able to recognize specific components (guest) and form aggregates held assembled through non-covalent interactions. During the last century, the theoretical bases of these weak attractive forces paved the way for the development of supramolecular chemistry.[1] More recently, the principle and methods of this new branch of chemistry have been applied to extend the concept of working devices and molecular machines to the molecular level.[2] A molecular machine can be defined as "an assembly of a discrete number of molecular components designed to perform mechanical-like movements (output) as a consequence of appropriate external energy (input)".[3] Within the plethora of examples of artificial molecular-level devices and machines, those belonging to the classes of pseudorotaxanes, rotaxanes, and catenanes[4] are among the more extensively employed because of their potential for the development of nanotechnology as, for example, logic molecular switching elements or as molecular motors.[5] The ability of these systems to work as molecular machines is due to the chemical information stored within their components.

A [n]pseudorotaxane is an intervowen complex in which a macrocycle (rota) acts as the host for a guest having an axial symmetry (axle) (Figure 1, the number of component species is indicated between square brackets before the name). [n] Rotaxanes and [n]catenanes are mechanically interlocked systems[6] in which two or more species are connected to each other, often by the presence of one or more stoppering moieties. Thus, since components could be separated only by breaking covalent bonds, these species are considered as a single chemical entity.[7] The threading process driving their formation is dictated by non-covalent interactions (i.e. hydrogen-bonding interactions) which are further responsible for their spatial rearrangement. The manipulation of these interactions through external stimuli can promote the reversible (and cyclic) dethreading-rethreading of the axle from/into

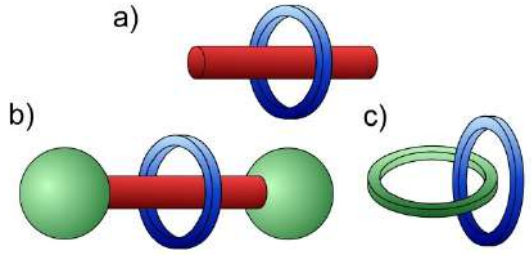


**Figure 1.** Schematic representation of a) a [2]pseudorotaxane complex, b) a [2]rotaxane, and c) a [2]catenane.

[a] *Prof. G. Cera, Prof. A. Arduini, Prof. A. Secchi*
Dipartimento di Scienze Chimiche, della Vita e della Sostenibilità Ambientale, Università di Parma, Parco Area delle Scienze 17/A, I-43124 Parma, Italy
E-mail: gianpiero.cera@unipr.it
arturo.arduini@unipr.it
andrea.secchi@unipr.it
[b] *Prof. A. Credi*
Dipartimento di Chimica Industriale "Toso Montanari", Viale del Risorgimento 4, I-40136 Bologna, Italy
E-mail: alberto.credi@unibo.it
[c] *Prof. A. Credi*
Istituto per la Sintesi Organica e la Foto reattività, Consiglio Nazionale delle Ricerche, via Gobetti 101, 40129 Bologna, Italy
[d] *Prof. S. Silvi*
Dipartimento di Chimica "G. Ciamician", Università di Bologna, Via Selmi 2, I-40126 Bologna, Italy
E-mail: serena.silvi@unibo.it

the wheel in pseudorotaxanes, the shuttling motion of the wheel along the axle in rotaxanes or the rotation of a cyclic component in a catenane (Figure 2).

These movements can thus mimic the functioning of a mechanical switch or a molecular machine. The construction of these systems and the study of their working mode have

Gianpiero Cera studied at the University of Bologna and completed his Ph.D. in 2014 at the same institute (with Prof. M. Bandini) working on gold catalysis. He then moved to the group of Prof. L. Ackermann at Georg-August-Universitat, Göttingen as an Alexander von Humboldt fellow, working on C–H functionalizations. In 2019, he was recruited as an assistant professor at the University of Parma. His main research activity is directed toward the development of supramolecular catalytic systems.

Arturo Arduini obtained his Laurea in Chemistry in 1981 under the supervision of Prof. G. Casnati, at the University of Parma where in 1983 he become assistant professor at the Istituto di Chimica Organica e Industriale. In 1989 he spent a period of research activity at the University of Twente (NL) under the supervision of Prof. D. N. Reinhoudt working on the regioselective functionalization of calixarenes. From 1998 he is associate professor of Organic Chemistry at the University of Parma. His current research interests include the design, synthesis and study of the properties of new working devices and prototype of molecular machines based on calixarenes.

Andrea Secchi completed his MSc (Honors) in Chemistry at the University of Parma. At the same University, he carried out his Ph.D. studies in Supramolecular Chemistry under Prof. A. Pochini. In 2001 he was a Visiting Scientist at the Centre d'Elaboration de Matériaux et d'Etudes Structurales (CEMES/CNRS) in Toulouse (France) under Dr. A. Gourdoun. Since 2010 is an Associate Professor of Organic Chemistry at the Department of Chemistry, Life Sciences and Environmental Sustainability of the University of Parma. His research interests span from calixarene chemistry, plasmonic metal nanostructures to NIR harvesting dyes.

Alberto Credi is professor of Chemistry at the University of Bologna and associate research director at Italy's National Research Council (CNR). He is the founder and scientific director of the Center for Light Activated Nanostructures (CLAN), a joint University-CNR laboratory for frontier research on light-responsive molecular-based devices, machines and materials. He has received several scientific awards, including an Advanced Grant from the European Research Council, and is the coauthor of over 300 scientific papers, reviews and book chapters, four monographs, and a handbook of photochemistry.

Serena Silvi got her MSc in 2002 at the University of Bologna with Prof. Vincenzo Balzani and in 2006 she earned her PhD under the supervision of Prof. Alberto Credi with a thesis on "Artificial Molecular Machines". In 2008 she was appointed at the Chemistry Department "Giacomo Ciamician" of the University of Bologna as assistant professor and in 2019 as associate professor. Her research activity is focused on the design and characterization of artificial molecular machines based on interlocked structures, photochromic compounds and photoactive molecular materials. She is the coordinator of a national research program on the development of photoresponsive host-guest functional systems in liposomes.

  

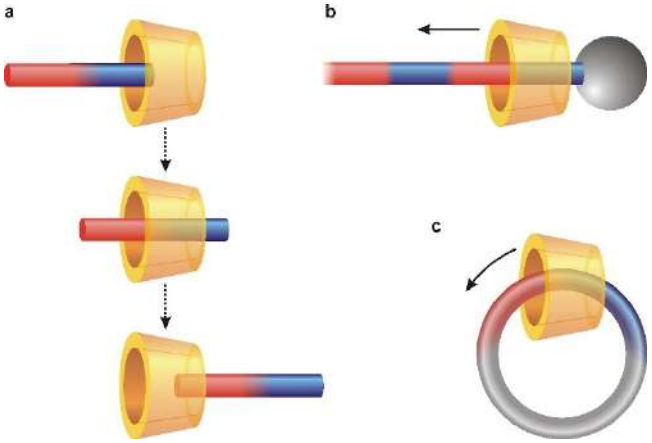


**Figure 2.** Representation of stimuli-controlled unidirectional threading/dethreading of a [2]pseudorotaxane (a), a processive linear motor based on a [2]rotaxane (b) and a rotary motor based on a [2]catenane (c). Image reproduced from Ref. [30]. Copyright © 2012 Wiley-VCH Verlag GmbH & Co. KGaA, Weinheim.

attracted the attention of many researchers over the years so that a wide variety of complementary components are now available that can be employed to build up molecular machines and devices based on these systems. As part of their ongoing research, several academic groups developed different synthetic routes to such structures with the final target to produce devices like switches, sensors, supramolecular catalysts, or active coating of solid surfaces. In this context, several supramolecular systems such as crown ethers, cyclodextrins, cucurbiturils, and calixarenes have been extensively exploited, and several books and reviews are now available that cover all the aspects relative to their chemistry (Figure 3).[8,9]

Calix[n]arenes present unique properties with respect to their parental supramolecular systems.[10] Unlike crown ethers and cucurbiturils, they are non-palindromic and synthetically versatile and represent a modular platform for the synthesis of heteroditopic receptors. Furthermore, in sharp contrast with water-soluble cyclodextrins that can form inclusion complexes via hydrophobic effect, their solubility in organic solvents and π-rich hydrophobic cavity allow calix[n]arenes to work smoothly in apolar organic media. These features render calix[n]arenes macrocycles a unique and versatile scaffold for the synthesis of pseudorotaxanes and rotaxanes itself.

During the last twenty years, our group focused its research on exploiting the modular reactivity of the calix[6]arene platform, to synthesize a new generation of calixarene-based devices and prototypes of molecular machines. Within this review, a survey of the significant achievements reported by our group, during two decades or so, will be described, guiding the reader toward a comprehensive and straightforward understanding of the supramolecular chemistry of triphenylureido-calix[6]arenes (Figure 4) mechanically interlocked molecules (MIMs).

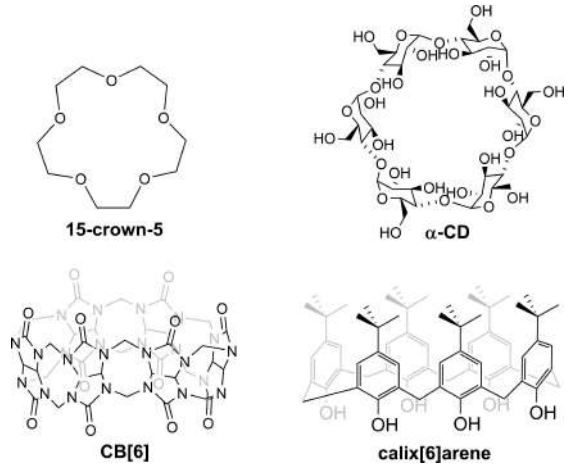


**Figure 3.** Representation of common supramolecular receptors.

## 2. Recognition Properties of TPU Wheel

The idea to employ calixarene derivatives as components of interlocked systems emerged in 1998 when it was envisaged by Vögtle and coworkers that the unique binding properties of these macrocycles could have been embedded into a rotaxane system.[11] Since then, synthetic strategies to obtain complex and topologically interesting mechanically locked dissymmetric capsules,[12] fourfold [2]rotaxanes,[13] and catenanes[14,15] have been identified. Following our precedent studies focused on the synthesis of self-assembled molecular cages based on calix[6]arene derivatives,[16,17] it was reported on the synthesis of the heteroditopic calix[6]arene receptor of type **1** bearing three phenylureido moieties able to extend the π-rich apolar cavity of the supramolecular object and to perform anion recognition.[18] Its ability to form inclusion complexes acting as

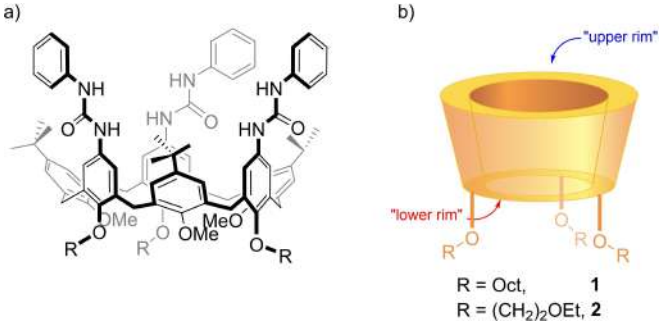


**Figure 4.** Triphenylureido calix[6]arene (**TPU**) motif (a) and its schematic counterpart (b).

  

a "molecular wheel" was subsequently evaluated by mixing **1** with dioctylviologen (DOV) salts **3** in $CDCl_3$ at 300 K (Scheme 1).[19]

$^1$H-NMR analysis highlighted a significant upfield shift (1 to 3 ppm) of aromatic C-*H* and N-C*H*$_2$ protons of the DOV axles **3a**, which indicated their inclusion in the cavity of the calix[6]arene wheel **1** with the formation of pseudorotaxanes (P) P[**1**⊃**3a**]2X. This shift is due to an anisotropic shielding effect applied by the π-rich aromatic cavity of the wheel on to the protons of the dicationic guest. Contemporary, N*H* signals of phenylureido groups suffered a substantial downfield shift indicating their engagement in hydrogen-bonding interactions with the corresponding counterions ($I^-$, $TsO^-$). From a spectroscopic point of view, the formation of these inclusion complexes was accompanied by a new, broad although weak UV-Vis absorption band at λ ≈460 nm, which could be attributed to charge-transfer interactions between the aromatic rings and bipyridium units. Hence, spectrophotometric titrations carried out in dichloromethane solution in the presence of axles **3a**•2OTs ($PF_6$) were employed to get more details in

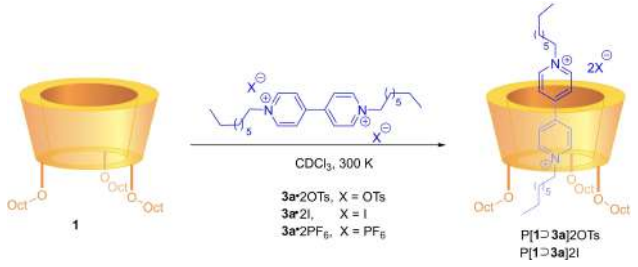


**Scheme 1.** Pseudorotaxanes formation through threading of DOV salts.

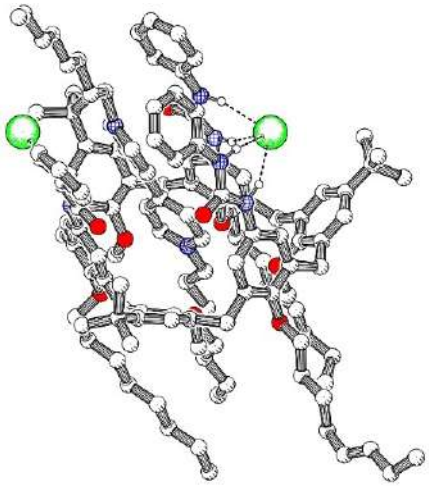

**Figure 5.** Pluton view of the X-ray crystal structure of pseudorotaxane P[**1**⊃**3a**]2I; hydrogen atoms except those involved in H-bonding have been omitted for clarity

the formation of pseudorotaxanes. The values of the apparent stability constant ($K_{st}$) are 6.0 and $0.8\times10^6$ $M^{-1}$ for [**1**⊃**3a**]2OTs and [**1**⊃**3a**]2$PF_6$, respectively.[20] This large difference clearly indicated that ion-pairing at the axle play an important role in the threading process and the larger stability of [**1**⊃**3a**]2OTs, despite the higher ion pair stability of TsO with respect to $PF_6$, suggested that counterions are, in fact, parts of the complex and contribute to its stabilization. X-ray diffraction analysis of complex [**1**⊃**3a**]2I further confirmed the nature of host-guest interactions (Figure 5).[19]

Subsequently, the features of calix[6]arene wheel **1** were employed for the synthesis of rotaxane (R) R[**1**⊃**4a**]2Br through a typical threading and stoppering reaction (Scheme 2).

These findings led soon to interrogate on the nature of the threading process and more precisely if the threading of the axle would involve the upper or the lower rim of the calix[6]arene wheel. To solve the riddle, unsymmetrical axles of type **5**•2OTs with a pre-installed stopper were synthesized, and both subsequently reacted in the presence of the wheel in apolar aromatic solvents.[21,22] It is noteworthy that $^1$H-NMR-analysis showed in both cases the selective formation of only one of the two possible pseudorotaxanes orientational isomers, and particularly, only those presenting the axle diphenylacetic stopper at the macrocycle upper rim P′[**2**⊃**5a**]2OTs and P′[**2**⊃**5b**]2OTs. This supported the hypothesis that threading of the axles proceeded selectively through the upper rim. Henceforth, the single quote after the P in the pseudorotaxane nomenclature indicates that a stoppered axle presents its stopper oriented toward the macrocycle upper rim while a double quote indicates the opposite pseudorotaxane orientational isomer (Scheme 3).

The results collected at this point of the investigation could be rationalized by considering these following different factors: i) in apolar solvents, the inward orientation at the NMR timescale of the three methoxy groups (see Figure 4a) of the calix[6]arene towards the cavity, disfavored the access of the axle through the lower rim by repulsive intermolecular

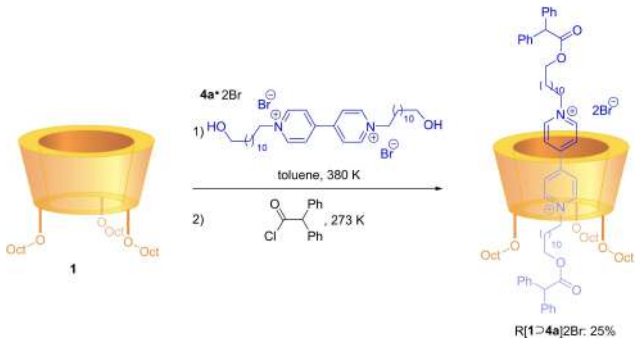


**Scheme 2.** Synthesis of rotaxane R[**1**⊃**4a**]2Br via stoppering reaction.

  

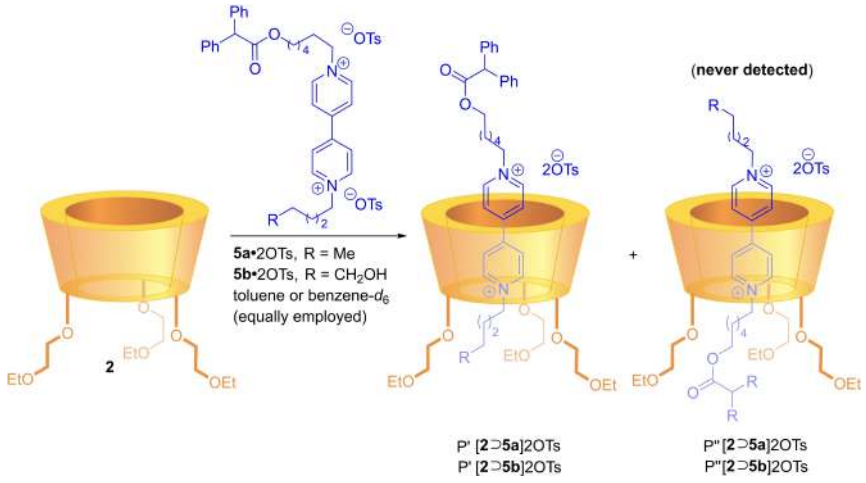


**Scheme 3.** Exploiting the unidirectional threading of axles **5** for the synthesis of oriented pseudorotaxane isomers.

interactions; ii) as evidenced by X-ray analysis, the size and binding ability of the wheel inner volume are suitable only for the inclusion of the cationic portion of the axle, leaving outside the cavity the corresponding counterions; iii) the hydrophilic ureido groups present at the wider rim of the calixarene play an important role as hydrogen-bond (HB)-donor groups and participate in the overall complexation process by ligating the two anions of the axle, pivoting the cationic portion of dialkyl viologen axles to thread exclusively from the upper rim of the wheel. Of course, in a scenario dominated by hydrogen-bonding interactions, secondary parameters such as the polarity of the solvent and temperature, have to play a crucial role in dictating the orientation of the threading process. In order to investigate their role in a more detailed manner, first the synthesis of pseudorotaxane P′[**2**⊃**5b**]2OTs was conducted in a polar solvent such as $CH_3CN$ (Scheme 4).[23]

Quite remarkably, a different product distribution was observed (1 : 2 ratio determined by NMR analysis of a crude mixture) in this case between P′/P″[**2**⊃**5b**]2OTs, demonstrating the threading of the axle to occur from the upper and the lower rim of the wheel. This trend seemed to be reasonable since polar solvents can compete with phenylureido groups by engaging hydrogen bonding (HB) with the tosylate counterions of the axle, limiting their pivotal role in controlling the directionality of the threading process. To get more insights on the enthalpies of the process, different axles of type **5** were synthesized and subsequently engaged in the threading process at different temperatures, using benzene-$d_6$ as the solvent. As expected, at 300 K, a monodirectional-oriented pseudorotaxane P' was observed in both cases (Scheme 5).

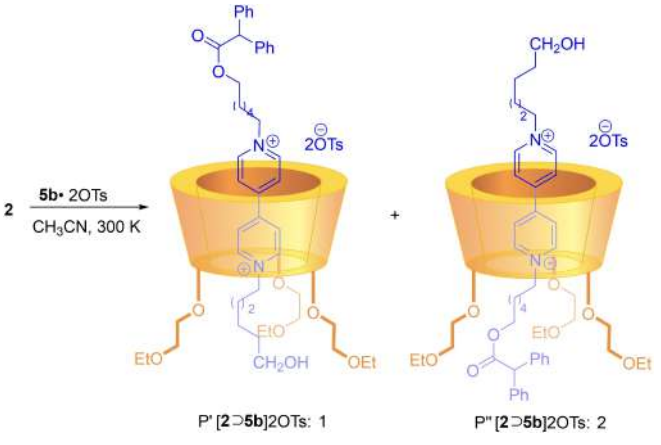


**Scheme 4.** Threading of axle **5b**•2OTs in $CH_3CN$.

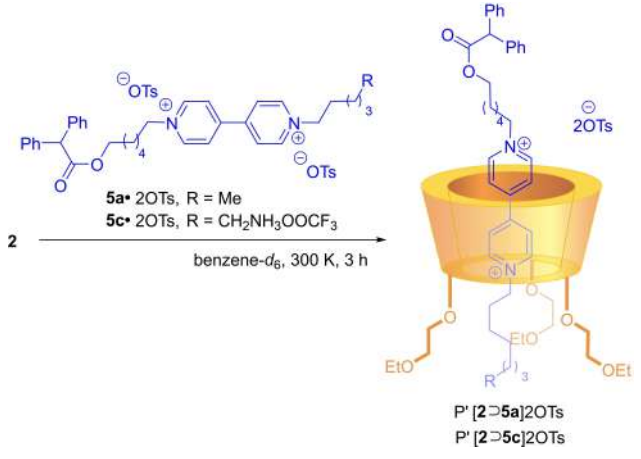


**Scheme 5.** Synthesis of monodirectional-oriented pseudorotaxane P′.

  

Subsequently, both pseudotoraxanes were heated up in an apolar media at 340 K (toluene-$d_8$ and benzene-$d_6$, respectively). While for P′[**2**⊃**5a**]2OTs, even after 7 days of refluxing, no isomerization was observed, P′[**2**⊃**5c**]2OTs underwent a product redistribution (P′/P"[**2**⊃**5c**]2OTs = 3 : 7) after only 12 h at 340 K. Hence, it became plausible that elements controlling the threading process in apolar media are no longer active in polar ones. To further study this possibility, an equimolar mixture of pseudorotaxanes P′/P"[**2**⊃**5a**]2OTs and P′/P"[**2**⊃**5c**]2OTs was obtained by performing the reaction in $CH_3CN$ at 300 K and re-dissolving the mixture in benzene-$d_6$ (clearly showing that multiple up- and down-oriented pseudorotaxanes have comparable thermodynamic stability in polar media). Subsequently, the two mixtures were both heated up at 340 K. While for solution of P′/P"[**2**⊃**5a**]2OTs, no notable difference in the product distribution was observed, the mixture P′/P"[**2**⊃**5c**]2OTs was detected in the same isomer ratio as observed in the reaction performed in $C_6D_6$ at 340 K (30 : 70, as for Scheme 6).[23]

In such a scenario, it is possible to argue that in apolar media, at 300 K, the threading process is under kinetic control and up-oriented rotaxanes are delivered as sole products. However, in the case of a positively charged amino group, the threading process could be under kinetic or thermodynamic control, depending on the solvent polarity, presumably thanks to secondary interactions between the charged amino group and phenylureido units. Based on what was observed in apolar media, the threading of the wheel by dialkylviologen axles occurs through the calix[6]arene upper rim mostly because phenylureido groups engage hydrogen bonding interactions with the tosylate counterions favoring the dissociation of the ion-pair. Hence, it became attractive to understand the threading of unsymmetrical dialkylviologen axles **6**•2OTs that can lead, in principle, to two different short and long oriented pseudo rotaxanes.[24] To this end, the case of four different axles was studied in benzene-$d_6$ at 300 K and the results collected (Scheme 7).

Interestingly, the selectivity of the threading process toward the $P'_{short}$ pseudorotaxane increases as the difference in the length of the two alkyl chains, with P[**1**⊃**6c**]2OTs and P[**1**⊃**6d**]2OTs affording exclusively the short-oriented isomers $P'_{short}$. Refluxing the mixtures, a redistribution up to 1 : 1 of the two orientational isomers was always observed for P[**1**⊃**6b**]2OTs and P[**1**⊃**6c**]2OTs, while the isomerization of P[**1**⊃**6d**]2OTs was only 20 % after the same time. A competition experiment to exploit the "length chain" selectivity was subsequently performed. Hence, a solution of **1** and an excess of symmetric axles **6e**•2OTs ($C_5C_5$) and **6f**•2OTs ($C_{18}C_{18}$) in an equimolar ratio was prepared in benzene-$d_6$. After 1 h of stirring, $^1$H-NMR analysis showed that pseudorotaxane P[**1**⊃**6e**]2OTs was the only species present in solution, highlighting once more not only how the threading process is governed by kinetics, but also that a simple alkyl chain could be used as a kinetic stopper to direct the unidirectional threading of the axle through the upper rim.

## 3. Template-assisted Synthesis of MIMs

The growing interest toward mechanically interlocked molecules (MIM) prompted several research groups to elaborate novel synthetic methodologies to deliver these supramolecular systems in a high efficient manner. Most of these approaches are based on the use of metal ions that are able to provide the correct spatial rearrangement of the precursors and eventually playing an active role in promoting the formation of covalent bonds that finally lead to MIMs.[25] In this context, electron-rich calixarene wheels of type **2** are able to form inclusion complexes with π-acceptors guests such as dialkyl viologen salts. Interestingly, the same trend was observed mixing a

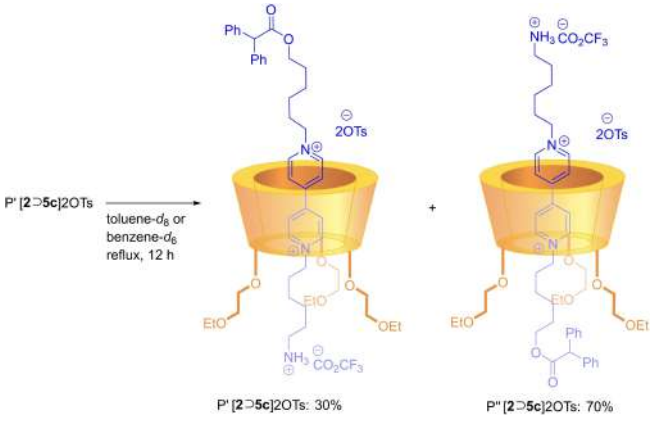


**Scheme 6.** Redistribution of P′[**2**⊃**5c**]2OTs at 340 K in aromatic apolar solvents

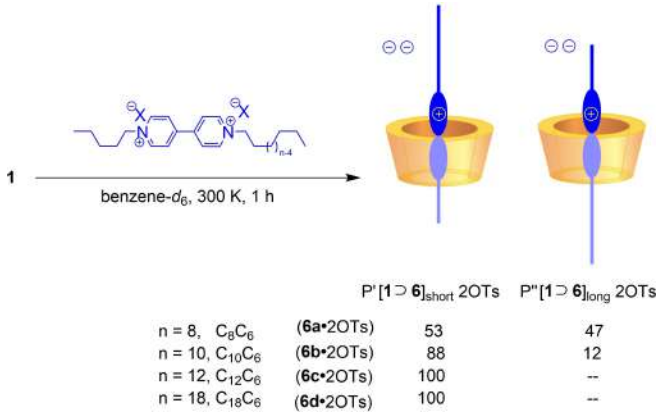


**Scheme 7.** Threading of unsymmetrical dialkylviologen axles of type **6**•2OTs.

  

pyridilpyridinium salt **7a**•OTs and triphenylureido calix[6]arene wheel in toluene. This paved the way for investigating on an unprecedented "metal-free" synthesis of oriented rotaxanes. Hence, NMR analysis performed in toluene-$d_8$ at 340 K, showed the formation of two distinct pseudorotaxanes isomers P′[**2**⊃**7a**]OTs and P"[**2**⊃**7a**]OTs (≅ 1 : 1 ratio) which differ for the relative orientation of their non-symmetrical components (Scheme 8).[26,27]

To verify this potential "template-assisted" effect, the mixture of pseudorotaxanes was treated with *n*-pentyl tosylate **8a** under different temperatures. Hence, pseudorotaxanes P′[**2**⊃**9a**]2OTs and P"[**2**⊃**9a**]2OTs were obtained as a 7 : 3 mixture at 340 K suggesting that the reaction takes place preferentially on P′[**2**⊃**7a**] which probably presents a more reactive nucleophilic site. Interestingly, the formation of P′[**2**⊃**9a**]2OTs is kinetically disfavoured; indeed, only P"[**2**⊃**9a**]2OTs is afforded performing the alkylation at room temperature. Kinetic analysis of the alkylation process fitted with a $S_N2$ type mechanism with a rate constant of $1.4 \times 10^{-4}\ s^{-1}$ for the reaction conducted with the calixarene wheel **2** and $8.6 \times 10^{-6}\ s^{-1}$ for the "un-assisted" one. These results highlighted that under present reaction conditions, the alkylation is 16 times faster when the calixarene is employed. To gain more insight into the mechanism of the reaction, we repeated the "template-assisted" alkylation with a series of pentyl derivatives **8** that differ for the leaving groups. As expected, the tosylate yielded the highest reaction rate and, in general, the results obtained for the entire series reflect the ability of the leaving groups (TsO > I > Br > Cl) present in the alkylating agent. This effect unequivocally highlighted the proximity effect of urea groups of the calixarene wheel that accelerated the $S_N2$ reaction by binding the anionic leaving group of the alkylating agents.[28] The "template-directed" approach was subsequently applied for the synthesis of oriented rotaxanes. This synthesis is traditionally accomplished by directional insertion of a 1,1-dialkyl-4,4-bipyridinium axle (possibly with one stoppered extremity) in the calixarene, followed by a stoppering (acylation) reaction. The rate-determining step of this approach is the alkylation of the bipyridine or pyridylpyridinium ion, which takes 7 days at reflux (Scheme 9, a). Hence, a more sustainable approach was realized by a supramolecular assisted strategy exploiting the different reactivities of oriented pseudorotaxanes (Scheme 9, b).

It is important to highlight that the novel strategy allowed for more sustainable synthesis of the two possible oriented rotaxanes with the longer chain facing the lower and the upper

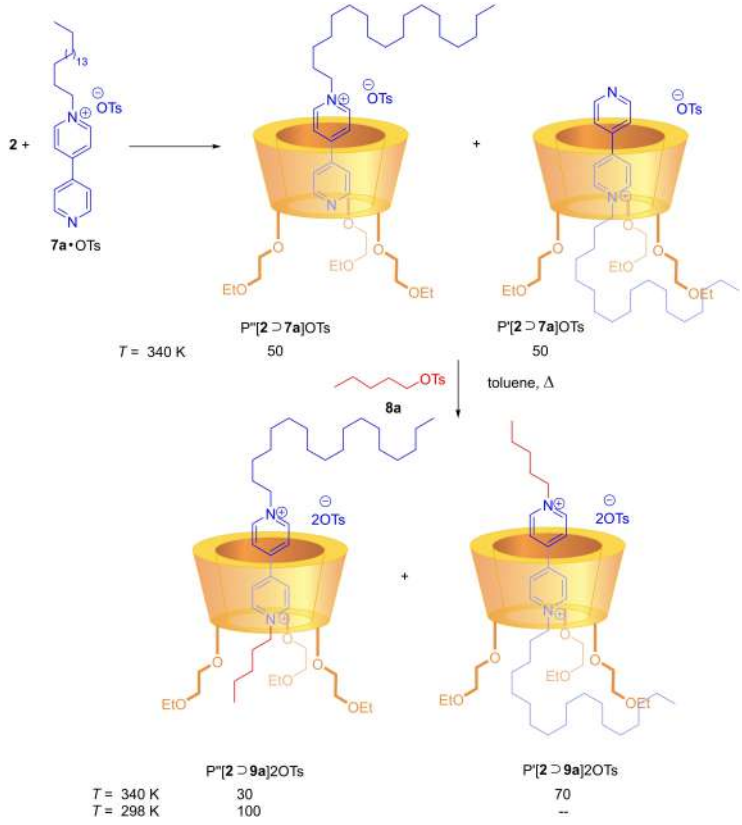


**Scheme 8.** Template-assisted approach for pseudorotaxane synthesis.

  

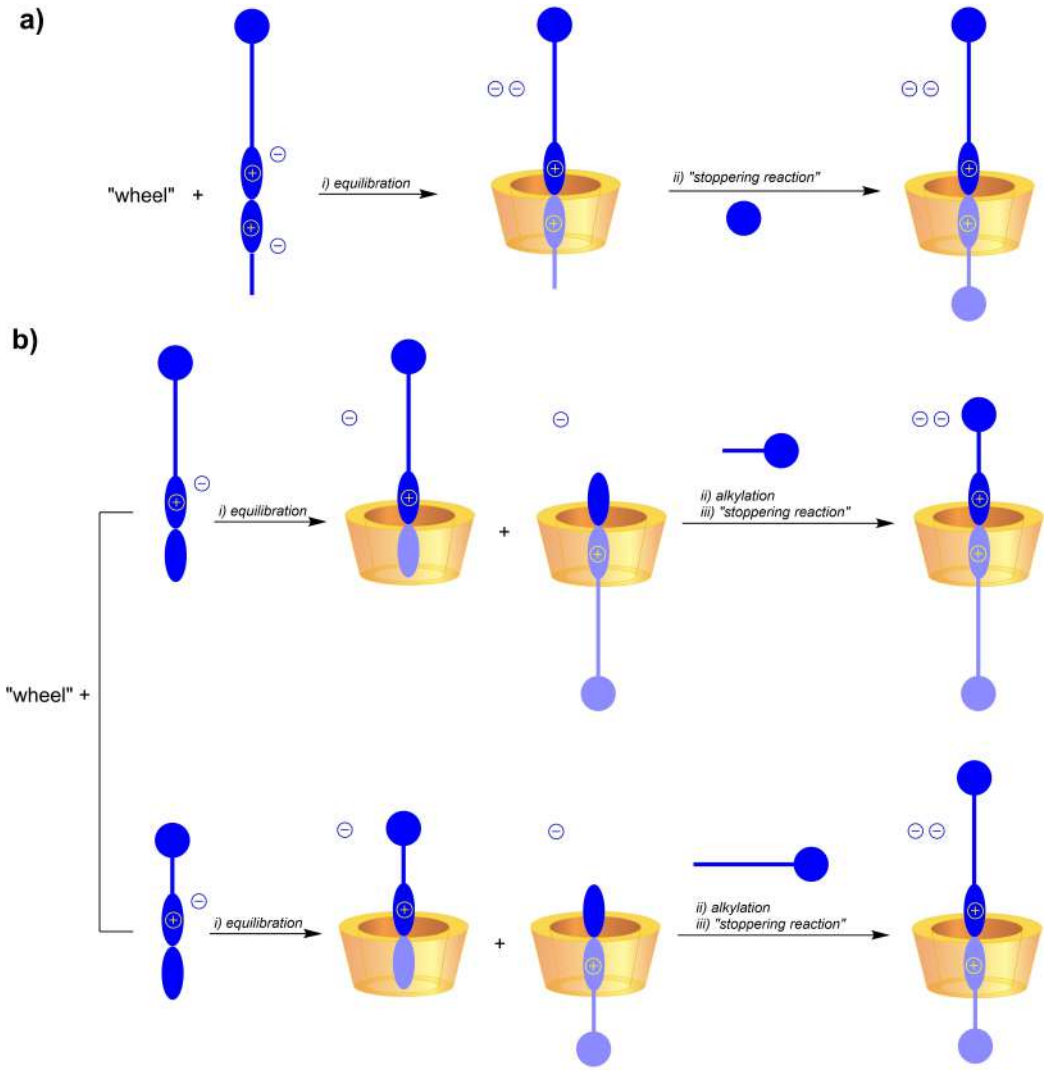


**Scheme 9.** Exploiting different approaches for rotaxane synthesis.

rim, respectively. This would be otherwise impossible to be realized using the traditional approach. Particularly, the equilibration of a pyridylpyridinium salt **7b**•OTs (whose synthesis requires only 24 h) with the wheel led to a 1 : 1 mixture of pseudorotaxanes P″/P′[**2**⊃**7b**]OTs (evaluated in toluene-$d_8$ at 340 K). This could be treated with 12-hydroxy-*n*-dodecyl tosylate **8b** in refluxing toluene for 4 days, enabling the selective formation of the oriented dicationic pseudorotaxane P′[**2**⊃**9b**]2OTs, that further delivers the corresponding rotaxane R′[**2**⊃**9b**]2OTs through a classical stoppering reaction (Scheme 10) in 63 % overall yield.

Through this approach, only rotaxane R′[**2**⊃**9b**]2OTs was formed, indicating unequivocally that only P′[**2**⊃**7b**]OTs underwent an accelerated alkylation reaction. All these evidence led us to conclude that a deep encapsulation of the pyridinium charge results in: i) a more exposed nucleophilic nitrogen at the upper rim; ii) a substantial change of the electron density of the axle that enhanced the nucleophilicity of the exposed nitrogen itself. These, along with urea moieties ability to stabilize the transition state by performing hydrogen bonding interactions, are suggestive of the "innate" selectivity of calixarene wheel in promoting a template-assisted synthesis of rotaxanes. To further prove the potentiality of the "wheel"-assisted reaction, the synthesis of catenanes was subsequently investigated. Hence, a "tailored-shape" symmetric dialkyl viologen axle **9c**•2OTs, that presents two terminal alkene units, was designed. Subsequently, equilibration of this axle with the calix[6]arene wheel **2** in toluene, followed by a well-established ring-closing metathesis (RCM) reaction using first-generation Grubb's catalyst (5 mol %, 298 K, 24 hs) led to

  

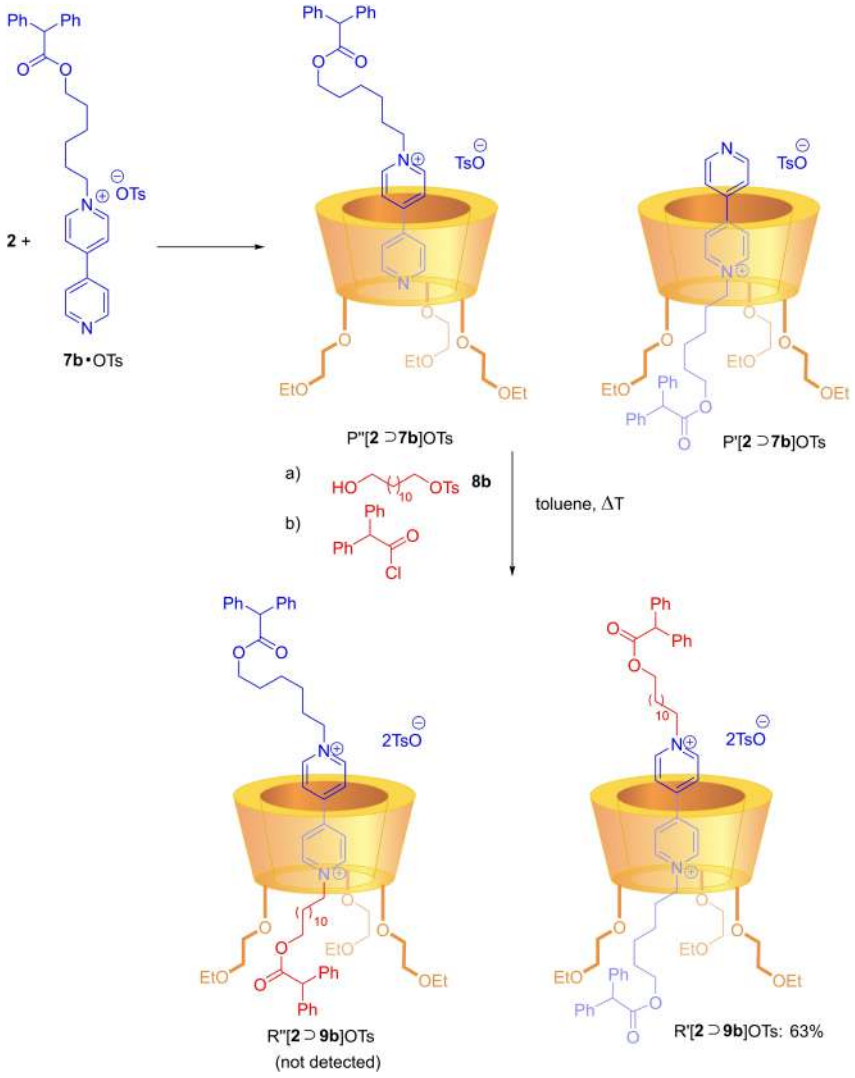


**Scheme 10.** Rotaxane synthesis via "template-assisted" approach.

catenane C[**2**⊃**9c**]2OTs in moderate yield (15%, Scheme 11).[29]

## 4. Stimuli-induced Rearrangements

### 4.1. Photocontrolled Dynamics

The development of molecular motors able to perform controlled threading/dethreading processes under external stimuli would represent an important advance toward the construction of "smart" materials. To address this issue, a specific class of axles bearing photoisomerizable stilbene units **10**•2OTs was synthesized (Scheme 12).[30]

Subsequently, rotaxanes R[**2**⊃**10a**]2OTs and R[**2**⊃**10b**]2OTs were synthesized under typical optimized reaction conditions at 273 K using diphenylacetyl chloride as the stoppering moiety. Detailed NMR analysis clearly showed the expected formation of sole up-oriented rotaxanes with the stilbene group positioned at the upper rim of the wheel. Further efforts were devoted to the study of the dethreading process. We hypothesized that the use of polar solvent such as DMSO would weaken secondary interactions that govern the threading process, favoring the slippage of the sufficiently thin stilbene-type unit from the lower rim of the wheel. Kinetics of dethreading process in polar solvents such as DMSO were further evaluated by monitoring the CT absorption band at 460 nm for both rotaxanes. Data fitting showed that the absorbance decay at $\lambda = 460$ nm takes place with a first-order kinetic law and with rate constants of $5.9 \times 10^{-3}$ and $9.3 \times 10^{-5}$ $s^{-1}$ for R[**2**⊃**10a**]2OTs and R[**2**⊃**10b**]2OTs, respec-

  

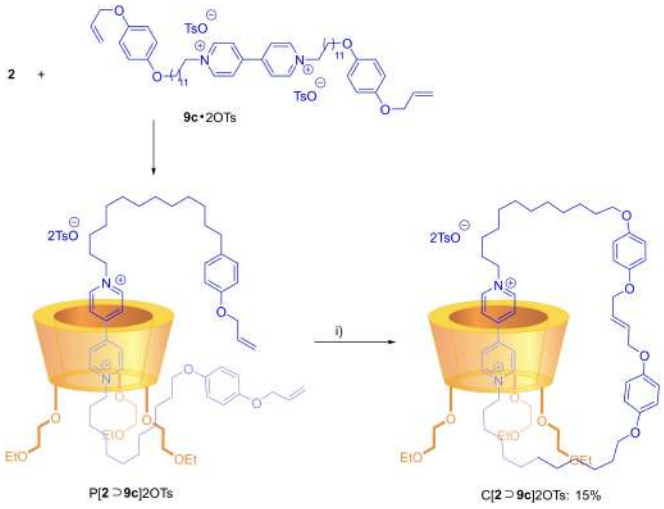


**Scheme 11.** Synthesis of catenane C[**2**⊃**9c**]2OTs by ring-closing metathesis.

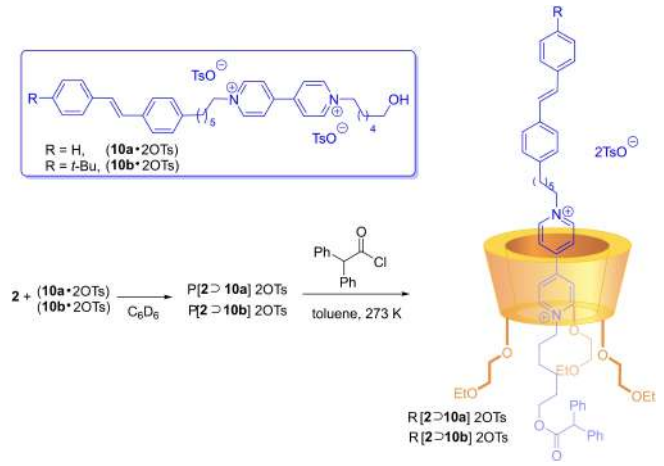


**Scheme 12.** Synthesis of up-oriented rotaxanes R[**2**⊃**10**]2OTs.

tively. The fact that the rate constants depend on the stilbene structure (unsubstituted and *t*-Bu-substituted) is a clear evidence that dethreading occurs through the slippage of this group from the lower rim of the wheel, upon dissolution in DMSO. The two orders of magnitude lower rate constant of R[**2**⊃**10a**]2OTs compared with R[**2**⊃**10b**]2OTs can indeed be explained on the basis of the higher steric hindrance of the *t*-Bu-substituted stilbene moiety (Scheme 13).

To further support the evidence of the unidirectional dethreading of the axle from the lower rim, the photocontrolled *cis*/*trans* isomerization of stilbene units was investigated. Both compounds, (*E*)-R[**2**⊃**10a**]2OTs and (*E*)-R[**2**⊃**10b**]2OTs, were irradiated for 90 min, causing about 70% conversion of the stilbene unit from the *E* to the *Z* isomer.

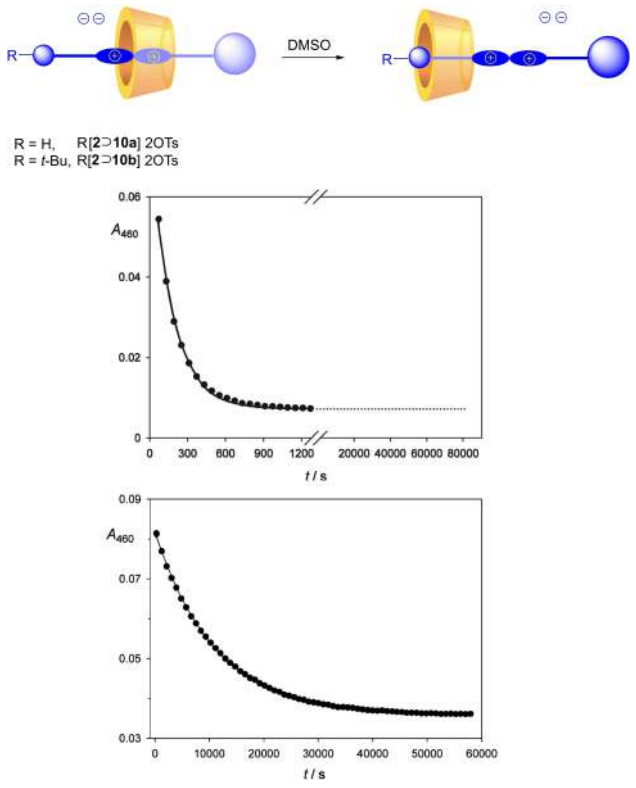


**Scheme 13.** Decrease of the CT absorption band at $\lambda = 460$ nm of compound R[**2**⊃**10a**]2OTs ($2.2 \times 10^{-4}$ M, top) and R[**2**⊃**10b**]2OTs ($2.3 \times 10^{-4}$ M, down) after dissolution in DMSO, at 298 K. Image partially adapted from Ref. [30]. Copyright © 2012 Wiley-VCH Verlag GmbH & Co. KGaA, Weinheim.

Subsequently, after evaporation of $CH_2Cl_2$, DMSO was added, and the CT absorption bands were monitored. As previously observed for the corresponding (*E*)-rotaxanes, the CT band decreased over time indicating the occurrence of axle dethreading also for the (*Z*)-R[**2**⊃**10a**]2OTs and (*Z*)-R[**2**⊃**10b**]2OTs. In the case of (*Z*)-R[2⊃**10a**]2OTs, the best fitting of the absorption values at $\lambda = 460$ nm clearly evidenced two superimposed first-order kinetics (Scheme 14, open circles) with rate constants of $5.9 \times 10^{-3}$ and $2.3 \times 10^{-5}$ $s^{-1}$, respectively.

The faster process, which accounts for 30% of the total decay, is attributed to the dethreading of the axle carrying the stilbene (*E*)-isomer because its rate constant coincides with the one obtained for non-irradiated rotaxane R[**2**⊃**10a**]2OTs. Intuitively, the slower process can be assigned to the dethreading of the axle comprising a (*Z*)-stilbene (note that no appreciable thermal *Z*-to-*E* isomerization was observed under examined conditions). The low value of its rate constant is in agreement with the higher hampering effect of the (*Z*)-isomer compared with the (*E*)-isomer, which results in a much more difficult dethreading of this unit from the wheel. It is interesting to notice that the *E*–*Z* photoisomerization affects

  

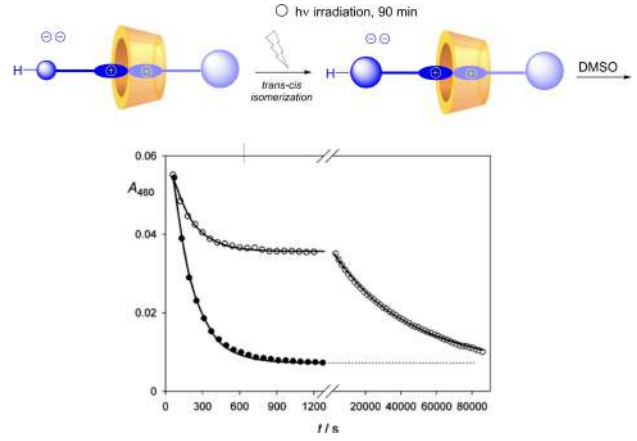


**Scheme 14.** Absorbance decrease at λ = 460 nm upon dissolution of (*E*)-R[**2**⊃**10a**]2OTs DMSO before (full circles) and after (open circles) exhaustive irradiation at λ = 334 nm. The first order fitting curves are also shown. Image partially adapted from Ref. [30]. Copyright © 2012 Wiley-VCH Verlag GmbH & Co. KGaA, Weinheim.

the dethreading rate constant more than the incorporation of the *tert*-butyl group on the stilbene unit (Scheme 15).

The rate constant observed upon isomerization is indeed about one order of magnitude slower than that observed in the case of the substituted stilbene. In the case of (*Z*)-R[**2**⊃**10b**]2OTs, a decrease of the CT absorption band of only about 30% is observed. The best fitting of the absorption values at λ = 460 nm (Scheme 15, open circles) highlights that this decrease occurs according to first-order kinetics with a rate constant of $4 \times 10^{-5}\ s^{-1}$, which is quite similar to the one obtained for dethreading of the non-irradiated (*E*)-R[**2**⊃**10b**]2OTs. It was concluded that the observed decay of the CT absorption band concerns the portion of the compound with

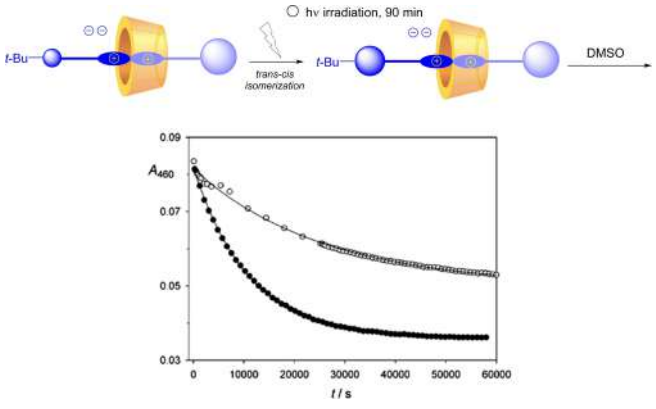


**Scheme 15.** Absorbance decrease at λ = 460 nm upon dissolution of (*E*)-(R[**2**⊃**10b**]2OTs DMSO before (full circles) and after (open circles) exhaustive irradiation at λ = 334 nm. The first order fitting curves are also shown. Image partially adapted from Ref. [30]. Copyright © 2012 Wiley-VCH Verlag GmbH & Co. KGaA, Weinheim.

the axle carrying the (*E*)-isomer of the *t*-Bu stilbene, and that the photoisomerized compound does not undergo dethreading, accounting for 70% of the CT absorption intensity that does not disappear in DMSO. Hence, our results show that the (*Z*)-isomer of the *t*-Bu stilbene is too bulky to pass through the lower rim of the wheel and that (*Z*)-R[**2**⊃**10b**]2OTs behaves like a real rotaxane. Overall, it was demonstrated for the first time that an external stimulus is able to promote the unidirectional transit of the axle through its wheel.

### 4.2. Redox-induced Dynamics

As dialkyl viologen salts are redox-active molecules, it became attractive to get insights on how the dynamics of threading/dethreading processes are influenced by the electrochemical state of the axles. Preliminary investigations by cyclic voltammetry and differential pulse voltammetry were conducted on a symmetric viologen salt **3a**•$2PF_6$ as the model substrate. This salt is characterized by two reversible monoelectronic reduction processes at −0.29 and −0.81 V and no oxidation process (with $TBAPF_6$ as the electrolyte, Figure 6a).[20] The inclusion of **3a**•$2PF_6$ into the cavity of **1** causes a large negative shift of the first reduction potential of the viologen unit of the axle (Figure 6b). In other words, the axle becomes more difficult to reduce, reflecting the stabilization offered by the wheel. The second reduction process of pseudorotaxane P[**1**⊃**3a**]$2PF_6$ occurs at the same potential as for the free axle (Figure 6b). These results show that one-electron reduction of **3a**•$2PF_6$ promotes its dethreading from **1**, in line with the behavior of several related bipyridinium-containing pseudorotaxanes. This process is further related to the fact that one-electron reduction decreases the π-acceptor and H-bonding donor abilities of the viologen unit, thereby destabilizing the pseudorotaxane structure.

Differently, rotaxane R[**1**⊃**4b**]$2PF_6$,[31,32] obtained with typical reaction conditions using a symmetric diol derivative **4b**•$2PF_6$, show two reversible or quasireversible monoelectronic reduction processes at more negative potential values with respect to the free bipyridinium derivative (Figure 6c). The reversibility of the electrochemical waves suggests that either no conformational rearrangement takes place, or the rearrangement is fast on the timescale of the electrochemical experiment. The shift toward negative potential values of the second reduction potential shows that the reduced forms of the bipyridinium still interact with the calix[6]arene. More detailed information was acquired by analyzing the absorption spectra of monoreduced DOV salt **3a**•2OTs and model rotaxane R[**1**⊃**4b**]2OTs (Figure 7).[32] The absorption spectra of monoreduced DOV salt **3a**•2OTs is characterized by two structured bands at $\lambda_{max} = 398$ and 602 nm both in the absence and in the presence of a calix[6]arene; the energy, shape and intensity of the bands are not perturbated by the presence of

  

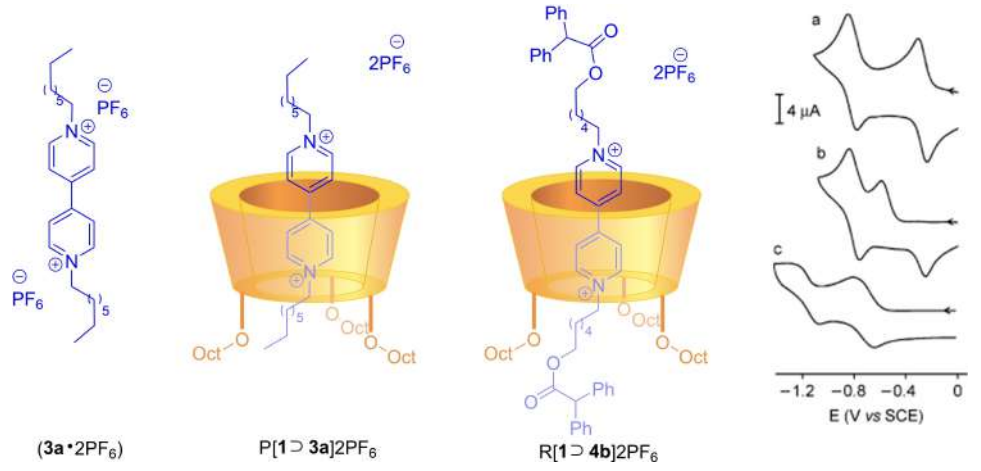


**Figure 6.** Cyclic voltammetric curves ($2\times10^{-4}$ M $CH_2Cl_2$ solution, 0.05 M $TBAPF_6$, 293 K; scan rate 0.2 $V s^{-1}$) for the first and second reduction of the viologen unit in (a) **3a**•2$PF_6$, (b) pseudorotaxane P[**1**⊃**3a**]2$PF_6$, (c) rotaxane R[**1**⊃**4b**]2$PF_6$. Image partially adapted from Ref. [20]. Copyright © 2004, American Chemical Society.

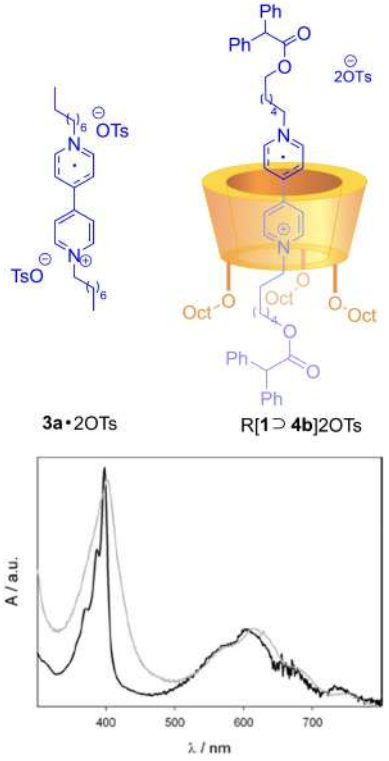


**Figure 7.** Absorption spectra of the radical cation species of DOV **3a**•2OTs (black) and R[**1**⊃**4b**]2OTs (gray). The spectra are normalized at the maximum of the lower energy band. Image partially adapted from Ref. [32]. Copyright © 2016 WILEY-VCH Verlag GmbH & Co. KGaA, Weinheim

the host, indicating that monoreduced pyridinium axle easily dethreads from the wheel. On the other hand, the spectrum of monoreduced rotaxane R[**1**⊃**4b**]2OTs features some significant differences. The band at higher energy is less structured while the band at lower energy is red-shifted. This indicated that axle **4b**•2OTs is still located in the cavity of the host even after mono reduction, although experiencing a different environment with respect to the free axle.

All these evidence led us to conclude that electrochemical stimulation of the bipyridinium core is not sufficient alone to induce any mechanical movement in rotaxanes. Hence, a second recognition site seemed to be necessary to facilitate displacement and promoting shuttling. To this goal, we envisaged the synthesis of two-station rotaxanes with an ammonium salt as a second unit that presents a different association strength with the calixarene receptor.[33] This would become a feasible approach to control the movement of wheels reversibly. Indeed, four different rotaxanes, depending on the position of the ammonium station (UP if the station is oriented towards the upper rim and DOWN if oriented toward the lower rim), were synthesized exploiting different strategies. In the first case, the presence of a bulky stopper able to selectively orient the threading process, lead smoothly to isolate rotaxane R-Up-short [**2**⊃**11a**]2OTs and R-Up-long [**2**⊃**11b**]2OTs after equilibration with wheel **2**, a second stoppering reaction and the final deprotection of the amino group (Scheme 16).

In the second case, a template-assisted synthesis was exploited using intermediates **11a′**(**b′**)•OTs and 6-bromohexyl 2,2-diphenylacetate **12**. This approach allows the alkylation of the pyridine ring facing the calixarene upper rim to proceed preferentially (see next session for more details). After equilibration, alkylation and final deprotection R-Down-short [**2**⊃**11a**]2OTs and R-Down-long [**2**⊃**11b**]2OTs could be obtained in moderate yields (Scheme 17).

  

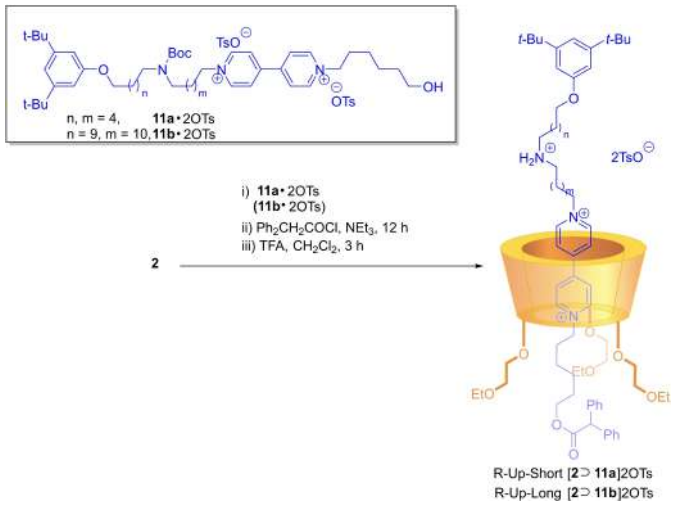


**Scheme 16.** Synthesis of R-Up-short [**2**⊃**11a**]2OTs and R-Up-long [**2**⊃**11b**]2OTs.

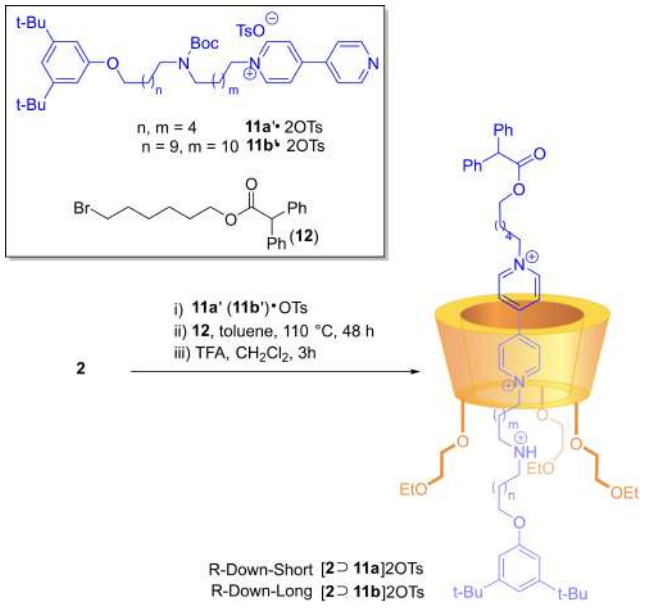


**Scheme 17.** Synthesis of R-Down-short [**2**⊃**11a**]2OTs and R-Down-long [**2**⊃**11b**]2OTs.

As previously concluded, in rotaxanes with single recognition sites, the electrochemical reduction of bipyridinium ring does not displace the ring from the station. Hence, it became attractive to study the electrochemical properties of previously synthesized two station rotaxanes R-Up/Down-short [**2**⊃**11a**]2OTs and R-Up/Down-long [**2**⊃**11b**]2OTs by cyclic voltammetry (CV) and different pulse voltammetry (DPV) (Table 1).

In line with previous studies, we could first observe that the first reduction potential of DOV **3a**•2OTs is comparable to those of dumbbells **11a**•2OTs and **11b**•2OTs, demonstrating that the electrochemical properties of bipyridinium axles are not influenced by the stoppers or the ammonium units. Conversely, the electrochemical potentials of rotaxanes [**2**⊃**11a/b**]2OTs are all shifted toward more negative values as a consequence of the stabilization of the axle provided by the electron-rich cavity of the calixarene. The second reduction potentials are, however, closer to the one of the uncomplexed axles suggesting that the calixarene ring moves away from the monoreduced bipyridinium unit. Further analysis of reduction potentials revealed a strong dependence on the length of the *N*-containing alkyl chains. Hence, the second reduction potentials of rotaxanes with shorter chains R-Up/Down-short [**2**⊃**11a**]2OTs are relatively higher than those of the corresponding long isomers. This suggests that the limited length of the axle causes weak, although not negligible, interactions between the calix[6]arene wheel and the ammonium as well as the bipyridinium stations. Moreover, rotaxane R-Down-short [**2**⊃**11a**]2OTs with a short *N*-containing chain, closer to the lower rim of the calixarene is easier to reduce with respect to all rotaxanes. This finding might be rationalized with a calixarene less engaged in charge-transfer interactions with the monoreduced bipyridinium unit, possibly because of pre-existing interactions with the ammonium site in its oxidized form. The voltammetric curves obtained for rotaxane R-Up-short [**2**⊃**11a**]2OTs were fitted by fixing the reduction potentials for the encapsulated and free species to the experimental values (Scheme 18). Overall, we could conclude that electrochemical stimulation of dipyridyl moiety, particularly its mono reduction, induces a mono-directional shuttling of the calixarene towards the more favored ammonium recognition site, allowing the complete reduction of the radical cation to its neutral form, outside the calixarene cavity.

The dynamics of supramolecular calix[6]arene systems were recently explored by our group with the synthesis of an artificial molecular lasso, able to self-assemble in low polar solvents, whose mechanical movement can be controlled by redox-stimulations.[34] The synthesis of calix[6]arene intermediate **13** was accomplished in satisfying yields, by a careful control of reaction conditions and particularly, playing with the stoichiometry of the reagents employed. Subsequently, after equilibration with dialkyl viologen salt **4b**•2OTs, catalytic amounts of TsOH were necessary to promote a transesterification reaction yielding [1]pseudorotaxane P[**13**⊃**4b**]2OTs in 65% yields. Interestingly, this structure could dimerize, depending on its concentration, to form a [c2]daisy chain structure. A typical stoppering reaction was crucial to re-equilibrate the system between the monomeric and dimeric structures, leading to the self-complexed [1]rotaxane R[**13**⊃**4b**]2OTs in a selective fashion (Scheme 19).

  

**Table 1.** Electrochemical potentials (vs. SCE) of the investigated compounds. Conditions: argon-purged acetonitrile, 0.04 M tetraethylammonium hexafluorophosphate, 30–40 mM analyte.

| Species[a] | | Reduction Potentials [V] E1 | E2 |
|---|---|---|---|
| DOV | **3a**•2OTs | −0.42 | −0.87 |
| DB-short | **11a**•2OTs | −0.41 | −0.85 |
| DB-long | **11b**•2OTs | −0.40 | −0.85 |
| R-Up-short | [**2**⊃**11a**]2OTs | −0.60 | −0.94 |
| R-Up-long | [**2**⊃**11b**]2OTs | −0.61 | −0.87 |
| R-Down-short | [**2**⊃**11a**]2OTs | −0.52 | −0.93 |
| R-Down-long | R[**2**⊃**11a**]2OTs | −0.60 | −0.88 |
| R–C6C6 | R[**1**⊃**3b**]2OTs | −0.64 | −1.15 |

The redox properties of these supramolecular structures were subsequently analyzed by cyclic voltammetry (CV) and compared with a typical free bipyridinium axle. For both species, the shift of the first reduction process to more negative potential values (−0.60 and −0.63 V, respectively), with respect to the one of DOV•2OTs (−0.41 V), highlighted how the mono-reduced species were still encapsulated and engaged in charge-transfer interactions. On the other hand, the second reduction potential for P[**13**⊃**4b**]2OTs (−0.88 V) is comparable to the one of the free-axle (−0.87 V) supporting the dethreading of the former from the wheel, leading to a hollow macrocyclic structure. The reversibility of the process was further confirmed by the chemical reversibility of the CV patterns and allowed the regeneration of the original lasso-like structure. The second reduction process is far more difficult for [1]rotaxane R[**13**⊃**4b**]2OTs with a potential of −1.18 V that is due to a stronger encapsulation enabled by a mechanical bond (Scheme 20).

### 4.3. Molecular Machines through Dynamic Control

The synthesis of a catenane through a template-assisted methodology encouraged our efforts toward the realization of a molecular machine. To this end, it is necessary to incorporate functional groups that could respond to different external stimuli leading to appropriate co-conformational rearrangements. Particularly, one of the most efficient approaches relies on the presence of two recognition sites on one ring (the 'track') for the other ring (the 'shuttle'); upon switching off and on the affinity of the primary site, the 'shuttle' ring moves onto and away from the secondary one, and reversible pirouetting can be achieved. An essential property for a molecular machine motor is the control of the directionality of the circumrotation; this might be addressed by rendering non-equivalent the clockwise and the anticlockwise direction, so the rotation in one direction is faster than the other one (Scheme 21). To investigate the dynamics of these supramolecular entities, we employed the strategy previously used for the synthesis of non-oriented [2]catenane C[**2**⊃**9c**]2OTs. Particularly, a non-symmetrical axle **14a**•2Br was designed and subsequently synthesized with a premeditatedly short alkyl chain to promote a directionally-controlled threading from the upper rim calix[6]arene wheel **2** (Scheme 22). After equilibration of axle **14a**•2Br in toluene at ambient temperature, a RCM reaction led to the isolation of the Boc-protected [2]catenane C[**2**⊃**14a**]2Br in 17% yields (Scheme 22, i). The final catenane C[**2**⊃**14b**]2Br was finally delivered by deprotection with TFA in quantitative yields (Scheme 22, ii).[35]

The electrochemical properties of oriented [2]catenane C[**2**⊃**14b**]2OTs was investigated by cyclic and differential pulse voltammetry techniques and compared with (a) the symmetrical one-station [2]catenane C[**2**⊃**9c**]2OTs, (b) the one-station rotaxane R[**2**⊃**4b**]2Br and (c) the free DOV **3a**•2OTs

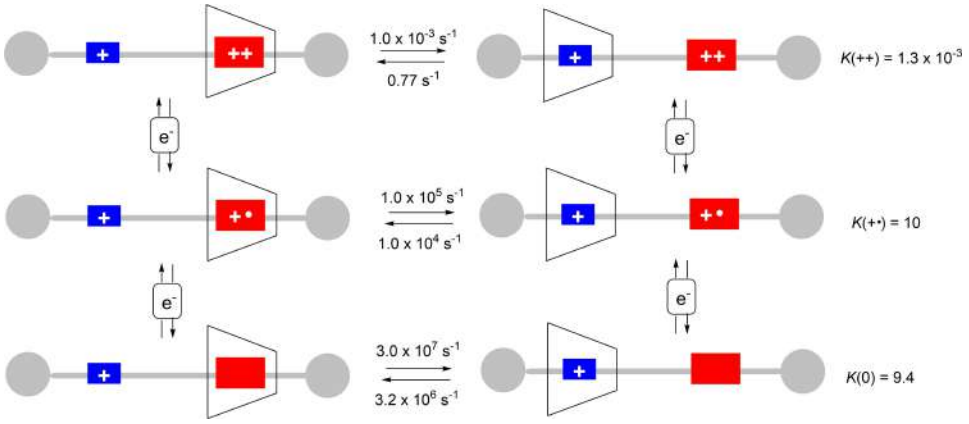


**Scheme 18.** Reaction scheme showing the thermodynamic and kinetic data for the simulated voltammogram of R-Up-short [**2**⊃**11a**]2OTs.

  

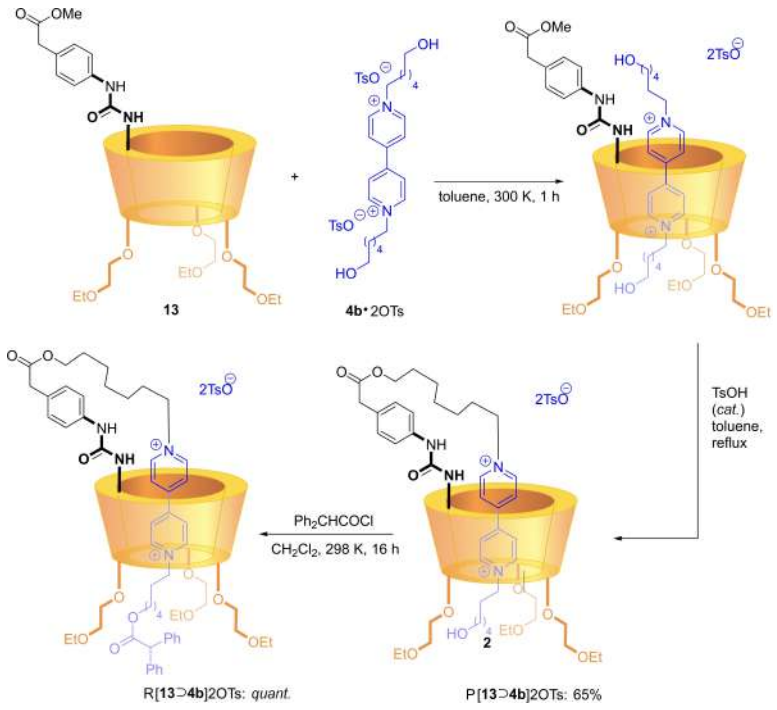


**Scheme 19.** Synthesis of calix[6]arene-based molecular lasso P[**13**⊃**4b**]2OTs.

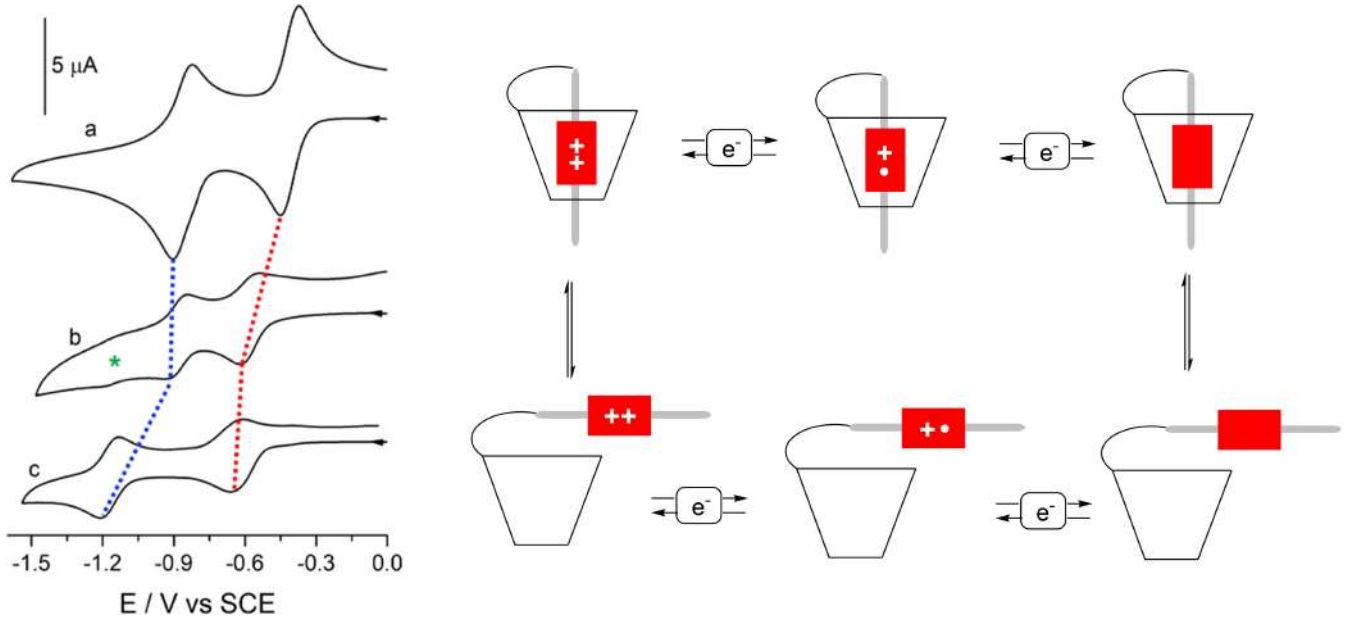


**Scheme 20.** Left: Cyclic voltammetry curves in $CH_3CN$ of DOV•2OTs ($2.4\times10^{-4}$ M), scan rate 100 mV/s (a), [1]pseudorotaxane P[**13**⊃**4b**]2OTs ($1.5\times10^{-4}$ M) (b), [1]rotaxane R[**13**⊃**4b**]2OTs ($1.8\times10^{-4}$ M) (c). Right: Schematic representation of the threading/dethreading equilibria and redox reactions of [1] pseudorotaxane P[**13**⊃**4b**]2OTs.

(Figure 8). Catenane C[**2**⊃**14b**]2OTs shows two reversible monoelectronic reduction processes at −0.597 and −0.877 V versus the standard calomel electrode (SCE) assigned to the first and second reduction of the bipyridinium unit, respectively (Figure 8a). Particularly, its first reduction potential is shifted toward more negative values with respect to the same

  

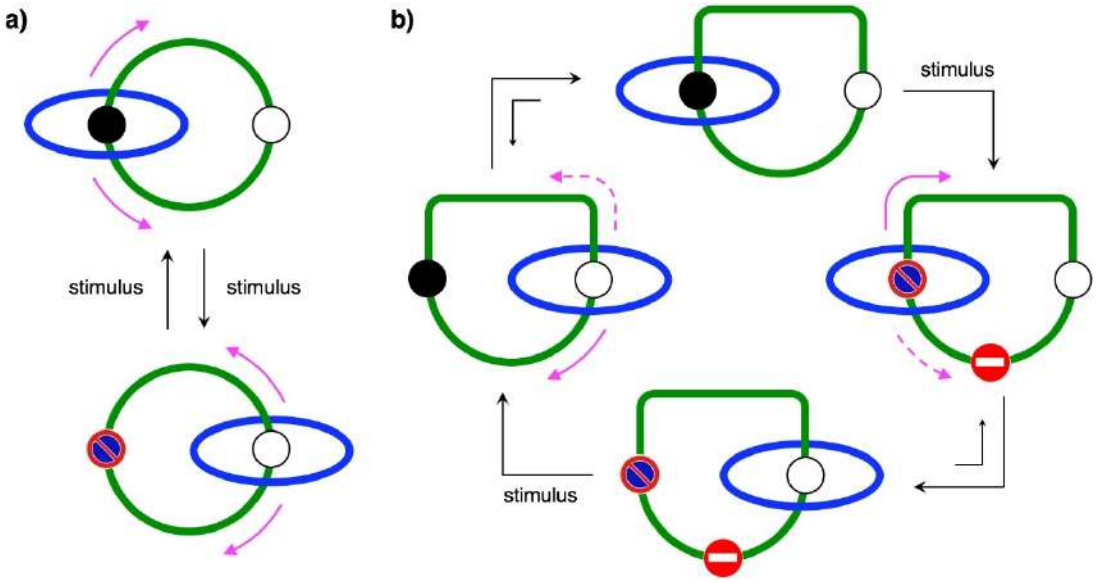


**Scheme 21.** (a) In a [2]catenane containing two different recognition sites on one ring, the relative rotation of the rings is achieved upon switching off and on the primary recognition site with an external stimulus. As the clockwise and anticlockwise directions are equally probable, no repetitive unidirectional circumrotation can be obtained. (b) In a bistable [2]catenane with an oriented 'track' ring, the clockwise and anticlockwise rotation directions are not equivalent. This is a key requirement for the construction of catenane rotary motors. Upon external modulation of both the relative affinities of the recognition sites and the shuttling barriers with a stimulus, full directional rotation of the blue ring around the "track" (e.g. clockwise as shown in the illustration) can be achieved. Dashed lines represent slow processes that are unlikely to occur. Image partially adapted from [34]. Reproduced by permission of The Royal Society of Chemistry.

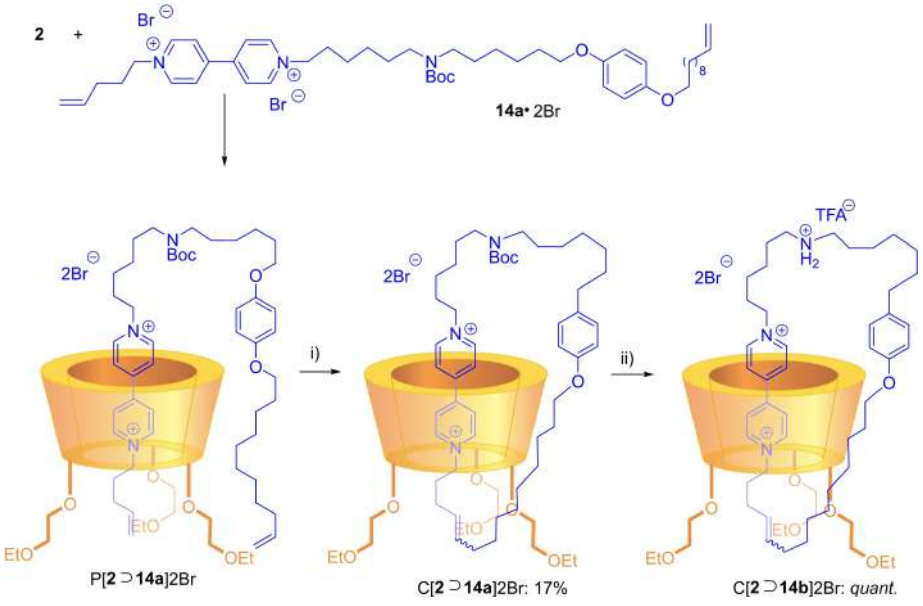


**Scheme 22.** Synthesis of catenane C[**2**⊃**14b**]2OTs by ring-closing methathesis.

process in the free DOV axle **3a**•2OTs. As previously described, this shift might be attributed to the stabilization provided by the π-rich cavity of **2**. In fact, the shift measured for catenane C[**2**⊃**14b**]2OTs is similar to that observed for other interlocked species such as C[**2**⊃**9c**]2OTs and R[**2**⊃**4b**]2Br, in which the bipyridinium unit is confined inside the aromatic cavity of **2**. However, the value of the second reduction potential of C[**2**⊃**14b**]2OTs is comparable to that of free DOV axle **3a**•2OTs (Figure 8b). This observation might be explained with the calixarene wheel not interacting

  

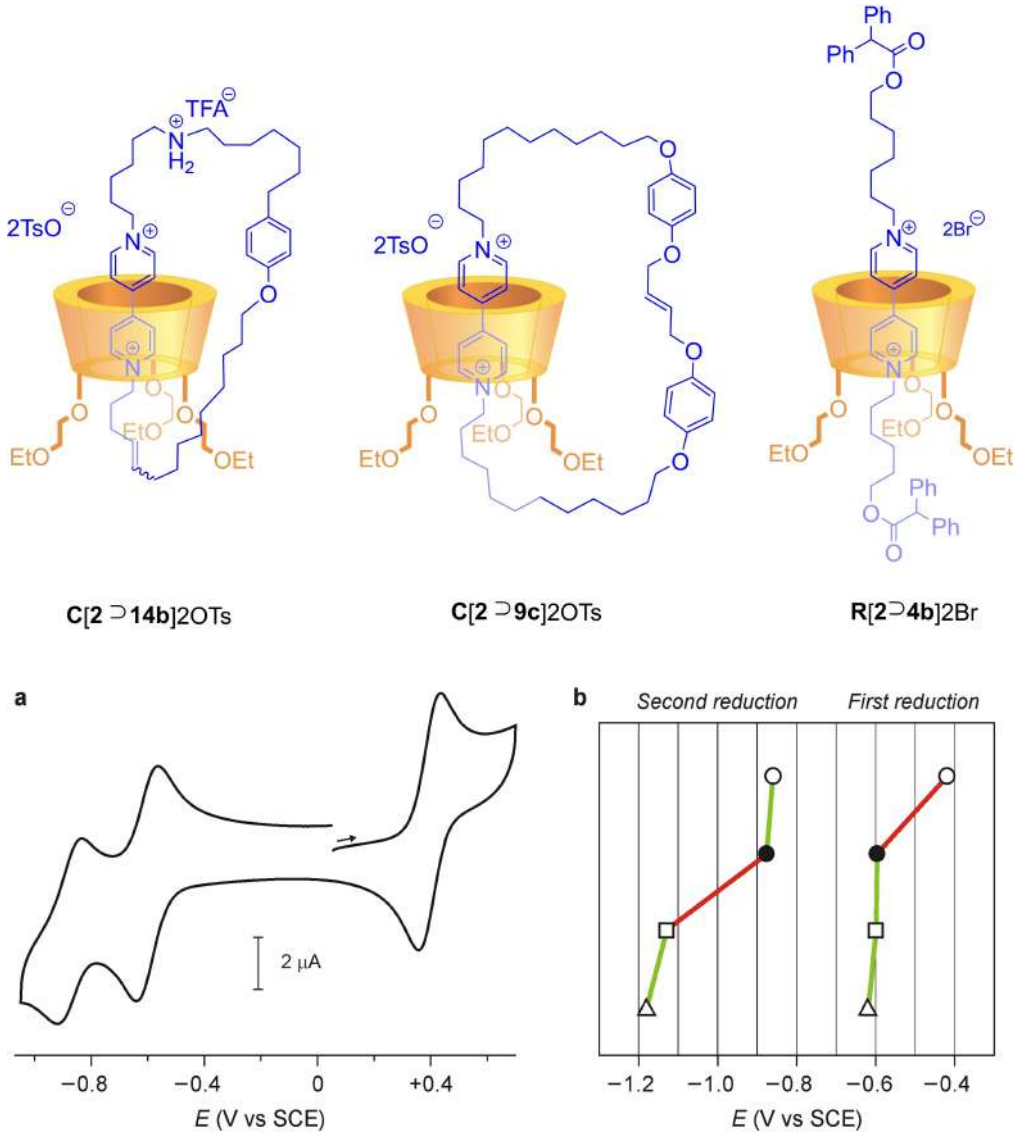


**Figure 8.** Electrochemical measurements: (a) Cyclic voltammogram of an argon-purged acetonitrile solution of catenane C[**2**⊃**14b**]2OTs (0.03 mM, 0.04 M tetraethylammonium hexafluorophosphate ($TEAPF_6$); scan rate 200 $mV s^{-1}$); the wave in the region of positive potentials is that of ferrocene used as an internal standard. (b) Genetic diagram for the first and second reduction processes for (from top to bottom): the free bipyridinium axle **3a**•2OTs (empty circles), the [2]catenane C[**2**⊃**14b**]2OTs (solid circles), the one-station [2]catenane C[**2**⊃**9c**]2OTs (squares); and the one-station [2]rotaxane R[**2**⊃**4b**]2Br (triangles). Image partially adapted from Ref. [35].

any longer with the monoreduced bipyridinium site, in sharp contrast to what was observed for the one-station catenane C[**2**⊃**9c**]2OTs. Hence, the presence of a second recognition unit enabled a translational movement of the calixarene ring upon one-electron reduction of the bipyridinium site. The full reversibility of all the voltammetric waves further confirmed the stability of the supramolecular system and that the re-oxidation of the bipyridinium site promoted the return of the calixarene, from the ammonium station to the dicationic unit.

Finally, calix[6]arenes are able to form stable pseudorotaxane complexes P[**1**⊃**7c**H]$PF_6$ ($K_{st} = 6 \pm 2 \times 10^6\ M^{-1}$) with axles obtained by simple protonation of pyridyl-pyridinium salts of type **7c**•$PF_6$. This property was finally exploited to design a molecular machine by coupling this complex with a second partner whose acid-base properties could be photo-controlled, specifically spyropyran photochrome SP (Scheme 23).[36]

The operating mode of this molecular machine could be rationalized as follows. In the dark, SP and pseudorotaxane

  

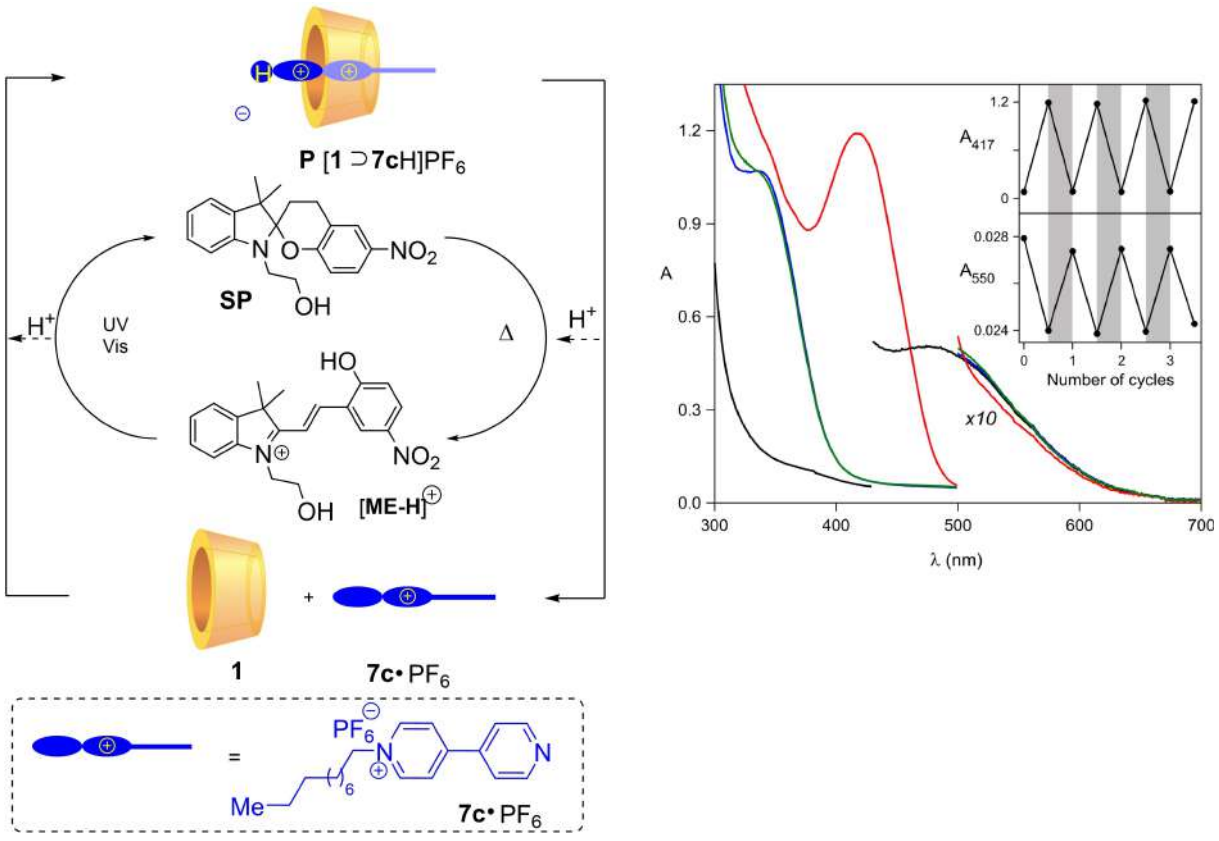


**Scheme 23.** Control of threading-dethreading processes in pseudorotaxane P[**1**⊃**7c**H]$PF_6$ by means of light-induced proton exchange with a spiropyran (SP)/merocyanine $[ME–H]^+$ photochromic system. (Right) absorption spectra in $CH_2Cl_2$ at RT of (i) P[**1**⊃**7c**H]$PF_6$ (black curve); (ii) P[**1**⊃**7c**H]$PF_6$ and SP, immediately after the addition of the latter (blue curve); (iii) solution (ii) after 7 days of rest in the dark (red curve); (iv) solution (iii) after 10 min of irradiation at $\lambda > 450$ nm (green curve). Inset: absorbance changes at 417 and 550 nm of $10^{-4}$ M solution of P[**1**⊃**7c**H]$PF_6$ and SP in $CH_2Cl_2$ taken upon several thermal equilibration cycles (white bars) and visible light irradiation (gray bars). Image partially adapted from Ref. [36]. Copyright © 2007, American Chemical Society

P[**1**⊃**7c**H]$PF_6$ are mixed as a solution of $CH_2Cl_2$ ($10^{-4}$ M) and a slow thermal proton transfer (7 days) from P[**1**⊃**7c**H]$PF_6$ to SP occurs, leading to the formation of merocyanine $[ME–H]^+$, that typically absorbs at $\lambda = 417$ nm, and dethreading of axle **7c**•PF6, which could be appreciated by a marked decrease of the CT band of the corresponding pseudorotaxane P[**1**⊃**7c**H]$PF_6$ at $\lambda = 478$ nm (red curve). Subsequently, light irradiation in the visible region of [ME–H]+ promotes the opposite proton transfer, regenerating pseudorotaxane P[**1**⊃**7c**H]$PF_6$, whose formation could be appreciated by the restoring of its typical CT absorption band (green curve). It appears evident that the photostationary resting state is shifted towards SP and pseudorotaxane P[**1**⊃**7c**H]$PF_6$, unless irradiation is carried out or temperature is increased, implementing a "memory" in the supramolecular system.

## 5. Future Perspectives and Outlook

A less exploited, yet intriguing possibility in supramolecular chemistry, that we are currently pursuing in our group, is the control of chemical and spectroscopic properties of organic molecules upon complexation. This would open new possibilities toward the synthesis of responsive function-oriented devices. In this context, we recently demonstrated the ability of calix[6]arene **2** wheel to tune the fluorescent properties of stilbazolium axles **15a**•OTs, depending on its relative orientation inside the macrocyclic cavity (Scheme 24).[37]

Yet, the modular platform was further explored through the synthesis of a new class of trisulfonamidecalix[6]arene derivatives of type **16**, that are able to work as Brönsted acid catalysts[38,39] and to form inclusion complexes with dialkylviologen salts **3**.[40] Intriguingly, we demonstrated how the features of the ion-pair associated to these axles are able to promote a selective conformational rearrangement in the corresponding pseudorotaxanes (Scheme 25).

  

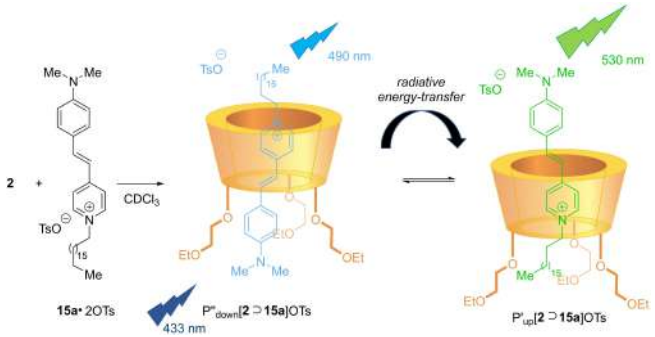


**Scheme 24.** Tuning the fluorescence through reorientation of the axle in calix[6]arene-based pseudorotaxanes.

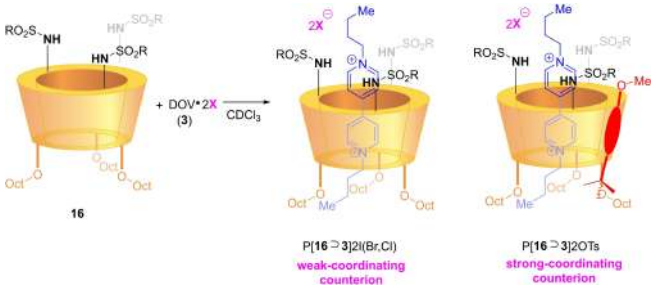


**Scheme 25.** Ion-pair selective conformational rearrangement of sulphonamidocalix[6]arene-based pseudorotaxanes.

Within this manuscript, we discussed how the functionalization of the upper and lower rim of calix[6]arene wheels allowed for the preparation of a platform of heteroditopic receptors, able to selectively recognize charged viologen-based guests, leading to supramolecular interwoven and interlocked structures.[41–49] The development of synthetic strategies to realize supramolecular species with a predetermined spatial orientation and the control of the directional motion of the relative threaded components is crucial to explore the still growing research area of calixarene-based nanodevices. In this context, further efforts will be directed towards the development of molecular machines able to store informations at the nanoscale level and stimuli-responsive catalysts.[45]

## *Acknowledgements*

This work was supported by the Italian Ministry of University and Research (PRIN 20173L7W8K and FARE R16S9XXKX3). Financial support from the EU (ERC AdG "Leaps" n. 692981) is gratefully acknowledged.

## References

[1] Supramolecular Chemistry, 8 Volume Set: From Molecules to Nanomaterials; J. W. Steed, P. A. Gale, Eds.; John Wiley & Sons, Ltd. **2012**.
[2] A. Credi, S. Silvi, M. Venturi, W. R. Browne, *Molecular Machines and Motors: Recent Advances and Perspectives*; A. Credi, S. Silvi, M. Venturi, Eds.; Topics in Current Chemistry Vol. 354; Springer International Publishing: Cham, **2014**; Vol. 354.
[3] C. J. Bruns, J. F. Stoddart, *The Nature of the Mechanical Bond: From Molecules to Machines*; John Wiley & Sons, Inc.: Hoboken, **2016**.
[4] J.-P. Sauvage, C. Dietrich-Buchecker, *Molecular Catenanes, Rotaxanes and Knots: A Journey Through the World of Molecular Topology*; J.-P. Sauvage, C. Dietrich-Buchecker, Eds.; Wiley-VCH Verlag GmbH: Weinhein, **2007**.
[5] J.-P. Sauvage, *Angew. Chem. Int. Ed.* **2017**, *56*, 11080–11093; *Angew. Chem.* **2017**, *129*, 11228–11242.
[6] Topology in Chemistry: Discrete Mathematics of Molecules; D. H. Rouvray, R. B. King, Eds.; Horwood Publishing Limited: Chichester, **2002**.
[7] J. W. Steed, D. R. Turner, K. J. Wallace, *Core Concepts in Supramolecular Chemistry and Nanochemistry*; John Wiley & Sons, Ltd: Chichester, **2007**.
[8] V. Balzani, M. Venturi, A. Credi, *Molecular Devices and Machines – A Journey into the Nanoworld*; Wiley-VCH Verlag GmbH: Weinheim **2003**.
[9] V. Balzani, A. Credi, M. Venturi, *Molecular Devices and Machines: Concepts and Perspectives for the Nanoworld: Second Edition*; Wiley-VCH Verlag GmbH: Weinheim, **2008**.
[10] M. Xue, Y. Yang, X. Chi, X. Yan, F. Huang, *Chem. Rev.* **2015**, *115*, 7398–7501.
[11] C. Fischer, M. Nieger, O. Mogck, V. Böhmer, R. Ungaro, F. Vögtle, *Eur. J. Org. Chem.* **1998**, *1998*, 155–161.
[12] M. Chas, P. Ballester, *Chem. Sci.* **2011**, *3*, 186–191.
[13] C. Gaeta, M. O. Vysotsky, A. Bogdan, V. Böhmer, *J. Am. Chem. Soc.* **2005**, *127*, 13136–13137.
[14] O. Molokanova, G. Podoprygorina, M. Bolte, V. Böhmer, *Tetrahedron* **2009**, *65*, 7220–7233.
[15] M. Janke, Y. Rudzevich, O. Molokanova, T. Metzroth, I. Mey, G. Diezemann, P. E. Marszalek, J. Gauss, V. Böhmer, A. Janshoff, *Nat. Nanotechnol.* **2009**, *4*, 225–229.
[16] A. Arduini, L. Domiano, L. Ogliosi, A. Pochini, A. Secchi, R. Ungaro, *J. Org. Chem.* **1997**, *62*, 7866–7868.
[17] A. Arduini, R. Ferdani, A. Pochini, A. Secchi, F. Ugozzoli, G. M. Sheldrick, P. Prados, J. J. González, J. de Mendoza, *J. Supramol. Chem.* **2002**, *2*, 85–88.
[18] J. J. González, R. Ferdani, E. Albertini, J. M. Blasco, A. Arduini, A. Pochini, P. Prados, J. de Mendoza, *Chem. Eur. J.* **2000**, *6*, 73–80.
[19] A. Arduini, R. Ferdani, A. Pochini, A. Secchi, F. Ugozzoli, *Angew. Chem. Int. Ed.* **2000**, *39*, 3453–3456; *Angew. Chem.* **2000**, *112*, 3595–3598.
[20] A. Credi, S. Dumas, S. Silvi, M. Venturi, A. Arduini, A. Pochini, A. Secchi, *J. Org. Chem.* **2004**, *69*, 5881–5887.
[21] A. Arduini, F. Calzavacca, A. Pochini, A. Secchi, *Chem. Eur. J.* **2003**, *9*, 793–799.

  

[22] A. Arduini, F. Ciesa, M. Fragassi, A. Pochini, A. Secchi, *Angew. Chem. Int. Ed.* **2005**, *44*, 278–281; *Angew. Chem.* **2005**, *117*, 282–285.
[23] A. Arduini, R. Bussolati, A. Credi, G. Faimani, S. Garaudée, A. Pochini, A. Secchi, M. Semeraro, S. Silvi, M. Venturi, *Chem. Eur. J.* **2009**, *15*, 3230–3242.
[24] A. Arduini, R. Bussolati, A. Credi, A. Secchi, S. Silvi, M. Semeraro, M. Venturi, *J. Am. Chem. Soc.* **2013**, *135*, 9924–9930.
[25] J. D. Crowley, S. M. Goldup, A.-L. Lee, D. A. Leigh, R. T. McBurney, *Chem. Soc. Rev.* **2009**, *38*, 1530–1541.
[26] G. Orlandini, G. Ragazzon, V. Zanichelli, A. Secchi, S. Silvi, M. Venturi, A. Arduini, A. Credi, *Chem. Commun.* **2017**, *53*, 6172–6174.
[27] Partial redistribution of pseudorotaxane isomers P′/P″[**2**⊃**7a**] OTs could be observed in toluene-$d_8$ after refluxing at 373 K for several hours.
[28] V. Zanichelli, G. Ragazzon, G. Orlandini, M. Venturi, A. Credi, S. Silvi, A. Arduini, A. Secchi, *Org. Biomol. Chem.* **2017**, *15*, 6753–6763.
[29] G. Orlandini, V. Zanichelli, A. Secchi, A. Arduini, G. Ragazzon, A. Credi, M. Venturi, S. Silvi, *Supramol. Chem.* **2016**, *28*, 427–435.
[30] A. Arduini, R. Bussolati, A. Credi, S. Monaco, A. Secchi, S. Silvi, M. Venturi, *Chem. Eur. J.* **2012**, *18*, 16203–16213.
[31] A. Arduini, R. Bussolati, A. Credi, A. Pochini, A. Secchi, S. Silvi, M. Venturi, *Tetrahedron* **2008**, *64*, 8279–8286.
[32] V. Zanichelli, G. Ragazzon, A. Arduini, A. Credi, P. Franchi, G. Orlandini, M. Venturi, M. Lucarini, A. Secchi, S. Silvi, *Eur. J. Org. Chem.* **2016**, *2016*, 1033–1042.
[33] V. Zanichelli, M. Bazzoni, A. Arduini, P. Franchi, M. Lucarini, G. Ragazzon, A. Secchi, S. Silvi, *Chem. Eur. J.* **2018**, *24*, 12370–12382.
[34] G. Orlandini, L. Casimiro, M. Bazzoni, B. Cogliati, A. Credi, M. Lucarini, S. Silvi, A. Arduini, A. Secchi, *Org. Chem. Front.* **2020**, *7*, 648–659.
[35] V. Zanichelli, L. Dallacasagrande, A. Arduini, A. Secchi, G. Ragazzon, S. Silvi, A. Credi, *Molecules* **2018**, *23*, 1156–1168.
[36] S. Silvi, A. Arduini, A. Pochini, A. Secchi, M. Tomasulo, F. M. Raymo, M. Baroncini, A. Credi, *J. Am. Chem. Soc.* **2007**, *129*, 13378–13379.
[37] M. Bazzoni, F. Terenziani, A. Secchi, G. Cera, I. Jabin, G. De Leener, M. Luhmer, A. Arduini, *Chem. Eur. J.* **2020**, *26*, 3022–3025.
[38] G. Cera, F. Cester Bonati, M. Bazzoni, A. Secchi, A. Arduini, *Org. Biomol. Chem.* **2021**, *19*, 1546–1554.
[39] G. Cera, D. Balestri, M. Bazzoni, L. Marchiò, A. Secchi, A. Arduini, *Org. Biomol. Chem.* **2020**, *18*, 6241–6246.
[40] G. Cera, M. Bazzoni, A. Arduini, A. Secchi, *Org. Lett.* **2020**, *22*, 3702–3705.
[41] V. Iuliano, C. Talotta, C. Gaeta, N. Hickey, S. Geremia, I. Vatsouro, V. Kovalev, P. Neri, *J. Org. Chem.* **2020**, *85*, 12585–12593.
[42] M. Tranfić Bakić, V. Iuliano, C. Talotta, S. Geremia, N. Hickey, A. Spinella, M. De Rosa, A. Soriente, C. Gaeta, P. Neri, *J. Org. Chem.* **2019**, *84*, 11922–11927.
[43] S. Moerkerke, V. Malytskyi, L. Marcélis, J. Wouters, I. Jabin, *Org. Biomol. Chem.* **2017**, *15*, 8967–8974.
[44] C. Talotta, N. A. De Simone, C. Gaeta, P. Neri, *Org. Lett.* **2015**, *17*, 4, 1006–1009.
[45] C. Gaeta, C. Talotta, P. Neri, *Chem. Commun.* **2014**, *50*, 9917–9920.
[46] C. Talotta, C. Gaeta, Z. Qi, C. A. Schalley, P. Neri, *Angew. Chem. Int. Ed.* **2013**, *52*, 7437–7441; *Angew. Chem.* **2013**, *125*, 7585–7589.
[47] R. Ciao, C. Talotta, C. Gaeta, L. Margarucci, A. Casapullo, P. Neri, *Org. Lett.* **2013**, *15*, 5694–5697.
[48] T. Pierro, C. Gaeta, C. Talotta, A. Casapullo, P. Neri, *Org. Lett.* **2011**, *13*, 2650–2653.
[49] C. Gaeta, F. Troisi, P. Neri, *Org. Lett.* **2010**, *12*, 2092–2095.
[50] M. Vlatković, B. S. L. Collins, B. L. Feringa, *Chem. Eur. J.* **2016**, *22*, 17080–17111.

*Manuscript received: January 18, 2021*
*Revised manuscript received: February 17, 2021*
*Version of record online: March 3, 2021*

  